BILEVEL OPTIMIZATION FOR CALIBRATING POINT SPREAD FUNCTIONS IN BLIND DECONVOLUTION

Michael Hintermüller and Tao Wu

Department of Mathematics, Humboldt-Universität zu Berlin
Unter den Linden 6, 10099 Berlin, Germany

(Communicated by Jun Zou)

Abstract. Blind deconvolution problems arise in many imaging modalities, where both the underlying point spread function, which parameterizes the convolution operator, and the source image need to be identified. In this work, a novel bilevel optimization approach to blind deconvolution is proposed. The lower-level problem refers to the minimization of a total-variation model, as is typically done in non-blind image deconvolution. The upper-level objective takes into account additional statistical information depending on the particular imaging modality. Bilevel problems of such type are investigated systematically. Analytical properties of the lower-level solution mapping are established based on Robinson's strong regularity condition. Furthermore, several stationarity conditions are derived from the variational geometry induced by the lower-level problem. Numerically, a projected-gradient-type method is employed to obtain a Clarke-type stationary point and its convergence properties are analyzed. We also implement an efficient version of the proposed algorithm and test it through the experiments on point spread function calibration and multiframe blind deconvolution.

1. **Introduction.** Image blur is widely encountered in many application areas; see, e.g., [6] and the references therein. In astronomy, images taken from a telescope appear blurry as light travels through a turbulent medium such as the atmosphere. The out-of-focus blur in microscopic images commonly occurs due to misplacement of the focal planes. Tomographic techniques in medical imaging, such as single-photon emission computed tomography (SPECT), are possibly prone to resolution limits of imaging devices or physical motion of patients, which both lead to blurring artifacts in final reconstructed images. In practice, the blurring operator, which can be modeled as the convolution with some *point spread function* (PSF) provided that the blurring is shift-invariant, is often not available beforehand and needs to be identified together with the underlying source image. Such a problem, typically known as *blind deconvolution* [33, 34], represents an ill-posed inverse problem in image processing, more challenging than non-blind deconvolution owing to the coupling of the PSF and the image.

There exists a diverse literature on blind deconvolution, which roughly divides into two categories: direct methods and iterative methods. The direct methods, such as the APEX method by Carasso [7, 8, 9, 10], typically assume a specific parametric structure on either the blurring kernel itself or its characteristic function, and are provably effective for specific applications. Among the iterative methods,

---

some use simple fixed-point type iterations, e.g. the Richardson-Lucy method [18], but their convergence properties and robustness against noise are difficult to analyze. Others proceed by formulating a proper variational model involving regularization terms on the image and/or the PSF. In [53] H^1-regularizations are imposed on both the image and the PSF, and in [13, 23] total-variation regularizations on the image and the PSF are utilized and yield better results than H^1-regularizations for certain PSFs. We also mention that nonconvex image priors are considered for blind deconvolution in the work [1], which are favorable for certain sparse images [14, 28, 29]. The convergence analysis of an alternating minimization scheme for such double-regularization based variational approaches in appropriately chosen function spaces is carried out in [4, 31]. An exception of variational approaches to blind deconvolution is [32], where the optimality condition is "diagonalized" by Fourier transform and thus can be solved by some non-iterative root-finding algorithm. Although we shall focus ourselves only on spatially invariant PSFs in this work, we remark that blind deconvolution with spatially varying PSFs might be advantageous in certain applications such as telescopic imaging; see, e.g., [3]. We also mention recent development in blind motion deblurring, which is a specific class of blind deconvolution; see, e.g., [36, 15, 49, 5].

Nevertheless, most existing variational approaches to blind deconvolution are "single-level", in the sense that both unknowns, i.e. the image and the PSF, appear in a single objective to be minimized. In this work, we are interested in a class of blind deconvolution problems where additional statistical information on the image (and possibly also on the PSF) is available. For instance, in microscopic imaging the blurring is nearly stationary and an artificial reference image can be inserted into the imaging device for obtaining a trial blurry observation of the reference image. In telescopic imaging, the target object, considered to be stationary, is photographed by multiple cameras within an instant, leading to highly correlated blurry observations. To exploit such additional image statistics, we propose a *bilevel optimization* framework. In essence, in the lower level the total-variation (TV) model (also known as the Rudin-Fatemi-Osher model [46]) is imposed as the constraint that the underlying source image must comply with, as is typically done in non-blind deconvolution [2, 12]. In the upper level, we minimize a suitable objective which incorporates the statistical information on the image and the PSF. Notably, bilevel optimization of similar structures has been recently applied to parameter/model learning tasks in image processing; see [35, 16].

Due to nonsmoothness of the objective in the (convex) TV-model, the sufficient and necessary optimality condition for the lower-level problem can be equivalently expressed as either a variational inequality, a nonsmooth equation, or a set-valued (or generalized) equation. This prevents us from applying the classical Karush-Kuhn-Tucker theory to derive a necessary optimality condition (or stationarity condition) for the overall bilevel optimization, and thus distinguishes our bilevel optimization problem from classical constrained optimization. Such difficulty is also typical in *mathematical programming with equilibrium constraints* (MPEC); see the monographs [38, 41] for comprehensive introductions on the subject. In this paper, we tackle the total-variation based bilevel optimization problem in the fashion of MPEC. For the lower-level problem, we justify the so-called *strong regularity condition* by Robinson [43] and then establish the B(ouligand)-differentiability of the solution mapping. Based on this, we derive the M(ordukhovich)-stationarity condition for the bilevel optimization problem. Yet, the C(larke)-stationarity, slightly

weaker than the M-stationarity, is pursued numerically by a hybrid projected gradient method and its convergence is analyzed in detail. In the numerical experiments, we implement a simplified version of the hybrid projected gradient method and demonstrate some promising applications on point spread function calibration and multiframe blind deconvolution.

The rest of the paper is organized as follows. We formulate the bilevel optimization model in section 2. In section 3, the lower-level solution mapping is studied in detail with respect to its existence, continuity, and differentiability. Different notions of stationarity conditions are introduced in section 4, where their relations are also discussed. Section 5 develops and analyzes a hybrid projected gradient method for pursuing a C-stationary point of the bilevel problem. Numerical experiments based on a simplified project gradient method are presented in section 6.

2. **A bilevel optimization model.** Let $u_{(\text{true})} \in \mathbb{R}^{|\Omega_u|}$ be the underlying source image over some two-dimensional (2D) index domain Ω_u. Assume the following image formation model for a blurry observation $z \in \mathbb{R}^{|\Omega_u|}$:

$$(1) \qquad z = K(h_{(\text{true})})u_{(\text{true})} + \text{noise}.$$

Here the noise is assumed to be white Gaussian noise. We denote by $\mathcal{L}(\mathbb{R}^{|\Omega_u|})$ the set of all continuous linear maps from $\mathbb{R}^{|\Omega_u|}$ to itself and assume that $K : h \in Q_h \mapsto K(h) \in \mathcal{L}(\mathbb{R}^{|\Omega_u|})$ is a given continuously differentiable mapping over a convex and compact domain Q_h in $\mathbb{R}^m$. In our theoretical and algorithmic development each $K(h)$ is only required to be a continuous linear operator on $\mathbb{R}^{|\Omega_u|}$, while in our numerics we focus on the cases where $K(h)$ represents a 2D convolution with some point spread function h, denoted by $K(h)u := h * u$. Thus, our task is to restore both unknowns, $u_{(\text{true})}$ and $h_{(\text{true})}$, from the observation z.

Whenever h is given, restoration of u (as non-blind deconvolution) can be carried out by solving the following variational problem:

$$(2) \qquad \text{minimize } \frac{\mu}{2}\|\nabla u\|^2 + \frac{1}{2}\|K(h)u - z\|^2 + \alpha\|\nabla u\|_1 \quad \text{over } u \in \mathbb{R}^{|\Omega_u|},$$

for some manually chosen parameters $\alpha > 0$ and $0 < \mu \ll \alpha$. Here $\nabla : \mathbb{R}^{|\Omega_u|} \to \left(\mathbb{R}^{|\Omega_u|}\right)^2$ is the discrete gradient operator with $\|\nabla u\|^2 = u^\top(-\Delta)u$, where Δ denotes the discrete Laplacian resulting from a standard five-point stencil (finite difference) discretization with homogenous Dirichlet boundary conditions. It is well-known that $-\Delta$ is symmetric and positive definite. Besides, $\|\cdot\|$ is the Euclidean norm in $\mathbb{R}^{|\Omega_u|}$ or $\left(\mathbb{R}^{|\Omega_u|}\right)^2$, and $\|\cdot\|_1$ is the ℓ^1-norm defined by $\|p\|_1 := \sum_{j\in\Omega_u} |p_j|$ for $p \in \left(\mathbb{R}^{|\Omega_u|}\right)^2$ where each $|p_j|$ is the Euclidean norm of the vector $p_j \in \mathbb{R}^2$. We also denote by $\langle\cdot,\cdot\rangle$ the standard inner product in $\mathbb{R}^2$, $\mathbb{R}^{|\Omega_u|}$, or $\left(\mathbb{R}^{|\Omega_u|}\right)^2$. The variational model (2) represents a discrete version of the Hilbert-space approach [30, 26] to total variation (TV) image restoration:

$$\text{minimize } \int_{\Omega_u} \left(\frac{\mu}{2}|\nabla u|^2 + \frac{1}{2}|K(h)u - z|^2 + \alpha|\nabla u|\right) dx \quad \text{over } u \in H_0^1(\Omega_u).$$

The problem (2) always admits a unique global minimizer due to the strict convexity of the objective. The associated sufficient and necessary optimality condition is given by the following *set-valued equation*:

$$(3) \qquad 0 \in F(u, h) + G(u),$$

where $F : \mathbb{R}^{|\Omega_u|} \times Q_h \to \mathbb{R}^{|\Omega_u|}$ and $G : \mathbb{R}^{|\Omega_u|} \rightrightarrows \mathbb{R}^{|\Omega_u|}$ are respectively defined as

(4) $\quad F(u,h) = (-\mu\Delta + K(h)^\top K(h))u - K(h)^\top z,$

(5) $\quad G(u) = \left\{ \alpha \nabla^\top p : p \in (\mathbb{R}^{|\Omega_u|})^2, \begin{cases} p_j = \frac{(\nabla u)_j}{|(\nabla u)_j|} & \text{if } j \in \Omega_u, \ (\nabla u)_j \neq 0 \\ |p_j| \leq 1 & \text{if } j \in \Omega_u, \ (\nabla u)_j = 0 \end{cases} \right\}.$

We remark that in the original work by Robinson [43] the term *generalized equations* was used for set-valued equations.

In this work, we propose a bilevel optimization approach to blind deconvolution. In an abstract setting, the corresponding model reads

(6) $\quad \begin{aligned} &\text{minimize (min)} \quad J(u,h) \\ &\text{subject to (s.t.)} \quad 0 \in F(u,h) + G(u), \\ &\qquad\qquad\qquad u \in \mathbb{R}^{|\Omega_u|}, \ h \in Q_h. \end{aligned}$

Here the TV model (2) represents the *lower-level problem* equivalently formulated as the first-order optimality condition (3), while in the *upper-level problem* we minimize a given objective $J : \mathbb{R}^{|\Omega_u|} \times Q_h \to \mathbb{R}$ known to be continuously differentiable and bounded from below. In this context, the set-valued equation (3) may be referred to as the *state equation* for the bilevel optimization (6), which implicitly induces a parameter-to-state mapping $h \mapsto u$.

3. **Solution mapping for lower-level problem: Existence, continuity, and differentiability.** In this section, we investigate the solution mapping associated with the lower-level problem in (6). To begin with, we establish the existence of such a solution mapping and its Lipchitz property by following Robinson's approach to set-valued equations [43]. In this context, the notion of the *strong regularity condition* [43] plays an important role. Essentially, the strong regularity condition for set-valued equations generalizes the invertibility condition in the classical implicit function theorem (for singled-valued equations), and thus allows the application of Robinsons generalized implicit function theorem; see [43, 17]. In Theorem 3.1, we justify the strong regularity condition at any feasible point and its consequence turns out to be far-reaching. In what follows, we write $D_u F(u,h)$ for the (partial) differential of F with respect to u.

Theorem 3.1 (Strong regularity and implicit function)**.** *The strong regularity condition* [43] *holds at any feasible solution* (u^0, h^0) *of* (3)*, i.e. the mapping* $w \in \mathbb{R}^{|\Omega_u|} \mapsto \{u \in \mathbb{R}^{|\Omega_u|} : w \in F(u^0, h^0) + D_u F(u^0, h^0)(u - u^0) + G(u)\}$ *is (globally) singled-valued and Lipschitz continuous. Consequently, there exists a locally Lipschitz continuous solution mapping* $S : h \mapsto u$ *such that* $u = S(h)$ *satisfies the set-valued equation* (3) *for all* h.

Proof. Due to Theorem 2.1 in [43], it suffices to show that the mapping $w \mapsto \{u \in \mathbb{R}^{|\Omega_u|} : w \in F(u^0, h^0) + D_u F(u^0, h^0)(u - u^0) + G(u)\}$ is globally singled-valued and Lipschitz continuous.

First, note that $F(u^0, h^0) + D_u F(u^0, h^0)(u - u^0) = (-\mu\Delta + K(h^0)^\top K(h^0))u - K(h^0)^\top z$. Then the single-valuedness follows directly from the fact that the mapping

$$0 \in (-\mu\Delta + K(h^0)^\top K(h^0))u - K(h^0)^\top z - w + G(u)$$

is the sufficient and necessary condition for the (strictly) convex minimization

$$\min_u \frac{\mu}{2}\|\nabla u\|^2 + \frac{1}{2}\|K(h^0)u - z\|^2 - \langle w, u \rangle + \alpha\|\nabla u\|_1,$$

which admits a unique solution.

To prove the Lipschitz property, consider pairs (u^1, w^1) and (u^2, w^2) that satisfy

$$0 \in (-\mu\Delta + K(h^0)^\top K(h^0))u^1 - K(h^0)^\top z - w^1 + G(u^1),$$
$$0 \in (-\mu\Delta + K(h^0)^\top K(h^0))u^2 - K(h^0)^\top z - w^2 + G(u^2).$$

Then there exist subdifferentials $p^1 \in \partial \|\cdot\|_1(\nabla u^1)$ and $p^2 \in \partial \|\cdot\|_1(\nabla u^2)$ such that

$$0 = (-\mu\Delta + K(h^0)^\top K(h^0))u^1 - K(h^0)^\top z - w^1 + \alpha\nabla^\top p^1,$$
$$0 = (-\mu\Delta + K(h^0)^\top K(h^0))u^2 - K(h^0)^\top z - w^2 + \alpha\nabla^\top p^2.$$

It follows from the property of subdifferentials in convex analysis, see e.g. Proposition 8.12 in [45], that

$$\|\nabla u^2\|_1 \geq \|\nabla u^1\|_1 + \langle p^1, \nabla u^2 - \nabla u^1 \rangle,$$
$$\|\nabla u^1\|_1 \geq \|\nabla u^2\|_1 + \langle p^2, \nabla u^1 - \nabla u^2 \rangle,$$

which further implies that

$$\langle p^1 - p^2, \nabla u^1 - \nabla u^2 \rangle \geq 0.$$

Thus, we have

$$0 = \langle (-\mu\Delta + K(h^0)^\top K(h^0))(u^1 - u^2) - (w^1 - w^2) + \alpha\nabla^\top(p^1 - p^2), u^1 - u^2 \rangle$$
$$\geq \langle (-\mu\Delta + K(h^0)^\top K(h^0))(u^1 - u^2), u^1 - u^2 \rangle - \langle w^1 - w^2, u^1 - u^2 \rangle,$$

and therefore the following Lipschitz property holds, i.e.

$$\|u^1 - u^2\| \leq \frac{1}{\lambda_{\min}(-\mu\Delta + K(h^0)^\top K(h^0))} \|w^1 - w^2\|,$$

where $\lambda_{\min}(\cdot)$ denotes the minimal eigenvalue of a matrix. This completes the proof. $\square$

In view of Theorem 3.1, we may conveniently consider the reduced problem

$$(7) \qquad \begin{aligned} \min \quad & \widehat{J}(h) := J(u(h), h) \\ \text{s.t.} \quad & h \in Q_h, \end{aligned}$$

which is equivalent to (6). It is immediately observed from (7) that there exists a global minimizer for (7) and thus also for (6).

Note that the state equation (3) can be expressed in terms of (u, h, p) as follows:

$$(8) \qquad \begin{cases} F(u, h) + \alpha\nabla^\top p = 0, \\ (u, \alpha\nabla^\top p) \in \text{gph} \, G, \end{cases}$$

where p is included as an auxiliary variable lying in the set

$$Q_p := \left\{ p \in (\mathbb{R}^{|\Omega_u|})^2 : |p_j| \leq 1 \; \forall j \in \Omega_u \right\},$$

and $\text{gph} \, G$ denotes the *graph* of the set-valued mapping G, i.e. $\text{gph} \, G = \{(u, v) : u \in \mathbb{R}^{|\Omega_u|}, v \in G(u)\}$. We call the triplet (u, h, p) a *feasible point* for (6) if (u, h, p) satisfies (8).

In the following, we briefly introduce notions from variational geometry such as tangent/normal cones and graphical derivatives. The interested reader may find further details in Chapter 6 of the monograph [45].

Definition 3.2 (Tangent and normal cones). The tangent (or contingent) cone of a subset Q in $\mathbb{R}^{|\Omega_u|}$ at $u \in Q$, denoted by $T_Q(u)$, is defined by

$$(9) \qquad T_Q(u) = \left\{ v \in \mathbb{R}^{|\Omega_u|} : t^k \to 0^+, \ v^k \to v, \ u + t^k v^k \in Q \ \forall k \right\}.$$

The (regular) normal cone of Q at $u \in Q$, denoted by $N_Q(u)$, is defined as the (negative) polar cone of $T_Q(u)$, i.e.

$$N_Q(u) = \left\{ w \in \mathbb{R}^{|\Omega_u|} : \langle w, v \rangle \le 0 \ \forall v \in T_Q(u) \right\}.$$

In our context, the tangent and normal cones of $\operatorname{gph} G$ can be progressively calculated as:

$$(10) \quad T_{\operatorname{gph} G}(u, \alpha \nabla^\top p) = \Big\{ (\delta u, \alpha \nabla^\top \delta p) : \delta u \in \mathbb{R}^{|\Omega_u|} \text{ and } \delta p \in (\mathbb{R}^{|\Omega_u|})^2 \text{ satisfy}$$
$$|(\nabla u)_j| \delta p_j = (\nabla \delta u)_j - \langle (\nabla \delta u)_j, p_j \rangle p_j, \quad \text{if } (\nabla u)_j \ne 0;$$
$$(\nabla \delta u)_j = 0, \ \delta p_j \in \mathbb{R}^2, \quad \text{if } |p_j| < 1;$$
$$\Big((\nabla \delta u)_j = 0, \ \langle \delta p_j, p_j \rangle \le 0 \Big) \vee \Big(\exists c \ge 0 : (\nabla \delta u)_j = c p_j, \ \langle \delta p_j, p_j \rangle = 0 \Big),$$
$$\text{if } (\nabla u)_j = 0, \ |p_j| = 1 \Big\}.$$

$$(11) \quad N_{\operatorname{gph} G}(u, \alpha \nabla^\top p) = \Big\{ (\alpha \nabla^\top w, -v) : w \in (\mathbb{R}^{|\Omega_u|})^2 \text{ and } v \in \mathbb{R}^{|\Omega_u|} \text{ satisfy}$$
$$\exists \xi_j \in \mathbb{R}^2 : w_j = \xi_j - \langle \xi_j, p_j \rangle p_j, \ (\nabla v)_j = |(\nabla u)_j| \xi_j, \quad \text{if } (\nabla u)_j \ne 0;$$
$$w_j \in \mathbb{R}^2, \ (\nabla v)_j = 0, \quad \text{if } |p_j| < 1;$$
$$\exists c \le 0 : \langle w_j, p_j \rangle \le 0, \ (\nabla v)_j = c p_j, \quad \text{if } (\nabla u)_j = 0, \ |p_j| = 1 \Big\}.$$

The directional differentiability of the solution mapping S invokes the following notion.

Definition 3.3 (Graphical derivative). Let $S : V \rightrightarrows W$ be a set-valued mapping between two normed vector spaces V and W. The graphical derivative of S at $(v, w) \in \operatorname{gph} S$, denoted by $DS(v, w)$, is a set-valued mapping from V to W such that $\operatorname{gph} DS(v, w) = T_{\operatorname{gph} S}(v, w)$, i.e.

$$\delta w \in DS(v, w)(\delta v) \quad \text{if and only if} \quad (\delta v, \delta w) \in T_{\operatorname{gph} S}(v, w).$$

Notably, when S is single-valued and locally Lipchitz near $(v, w) \in \operatorname{gph} S$ and $DS(v, w)$ is also singled-valued such that $\delta w = DS(v, w)(\delta v)$, one infers that S is directionally differentiable at v along δv with the directional derivate $S'(v; \delta v) = \delta w$; see, e.g., [37]. The directional differentiability of the lower-level solution mapping S is asserted in the following theorem.

Theorem 3.4 (Directional differentiability). *Let* $S : Q_h \to \mathbb{R}^{|\Omega_u|}$ *be the solution mapping in Theorem 3.1 and* (u, h, p) *be a feasible solution satisfying the state equation (8). Then* S *is directionally differentiable at* h *along any* $\delta h \in T_{Q_h}(h)$. *Moreover, the directional derivative* $\delta u := S'(h; \delta h)$ *is uniquely determined by the following sensitivity equation:*

$$(12) \qquad \begin{cases} D_u F(u, h) \delta u + D_h F(u, h) \delta h + \alpha \nabla^\top \delta p = 0, \\ (\delta u, \alpha \nabla^\top \delta p) \in T_{\operatorname{gph} G}(u, \alpha \nabla^\top p). \end{cases}$$

Proof. By [50, Theorem 4.1], the following estimate on the graphical derivative of S holds true:
(13)
$$DS(h, u)(\delta h) \subset \left\{ \delta u \in \mathbb{R}^{|\Omega_u|} : 0 \in D_u F(u, h)\delta u + D_h F(u, h)\delta h + DG(u, -F(u, h))(\delta u) \right\}.$$

With the introduction of the auxiliary variables p and δp such that (u, h, p) satisfies (8) and $(\delta u, \alpha \nabla^\top \delta p) \in T_{\mathrm{gph}\, G}(u, \alpha \nabla^\top p)$, the relation (13) is equivalent to
(14)
$$DS(h, u)(\delta h) \subset \left\{ \delta u \in \mathbb{R}^{|\Omega_u|} : (\delta u, \delta h, \delta p) \text{ satisfies the sensitivity equation (12)} \right\}.$$

Let $\delta h \in T_{Q_h}(h)$ be arbitrarily fixed in the following.

We first show that the set $DS(h, u)(\delta h)$ is nonempty. Following the definition of a tangent cone in (9), there exists $t^i \to 0^+$, $\delta h^i \to \delta h$ such that $h + t^i \delta h^i \in Q_h$ for all i. Then we have
$$\limsup_{i \to \infty} \frac{\|S(h + t^i \delta h^i) - S(h)\|}{t^i} \le \kappa \|\delta h\|,$$

where κ is the Lipschitz constant for S near h. As a result, possibly along a subsequence, we have
$$\lim_{i \to \infty} \frac{S(h + t^i \delta h^i) - S(h)}{t^i} = \delta u$$

for some $\delta u \in \mathbb{R}^{|\Omega_u|}$. Thus, we assert that $(\delta h, \delta u) \in T_{\mathrm{gph}\, S}(h, u)$, or equivalently $\delta u \in DS(h, u)(\delta h)$.

Next we show that δu must be unique among all solutions $(\delta u, \delta p)$ for (12). Fixing $h \in Q_h$, let $(\delta u^1, \delta p^1)$ and $(\delta u^2, \delta p^2)$ be two solutions for (12). Then we have
$$D_u F(u, h)(\delta u^1 - \delta u^2) + \alpha \nabla^\top (\delta p^1 - \delta p^2) = 0,$$

which further implies
$$\langle \delta u^1 - \delta u^2, D_u F(u, h)(\delta u^1 - \delta u^2) \rangle + \alpha \langle \nabla \delta u^1 - \nabla \delta u^2, \delta p^1 - \delta p^2 \rangle = 0.$$

We claim that $\langle \nabla \delta u^1 - \nabla \delta u^2, \delta p^1 - \delta p^2 \rangle \ge 0$. Indeed, we component-wisely distinguish the following three cases.

(1) Consider $j \in \Omega_u$ where $|p_j| < 1$. Then it follows immediately from (10) that $(\nabla \delta u^1)_j - (\nabla \delta u^2)_j = 0$.

(2) Consider $j \in \Omega_u$ where $(\nabla u)_j \ne 0$. Then from (10) we have
$$\langle (\nabla \delta u^1)_j - (\nabla \delta u^2)_j, \delta p_j^1 - \delta p_j^2 \rangle$$
$$= \langle (\nabla \delta u^1)_j - (\nabla \delta u^2)_j, \frac{1}{|(\nabla u)_j|}(I - p_j p_j^\top)((\nabla \delta u^1)_j - (\nabla \delta u^2)_j) \rangle$$
$$\ge \frac{1}{|(\nabla u)_j|}(1 - |p_j|^2)|(\nabla \delta u^1)_j - (\nabla \delta u^2)_j|^2 \ge 0.$$

(3) The last case where $j \in \Omega_u$ with $(\nabla u)_j = 0$ and $|p_j| = 1$ further splits into three subcases.
  (3a) Consider $(\nabla \delta u^1)_j = 0$, $\langle \delta p_j^1, p_j \rangle \le 0$ and $(\nabla \delta u^2)_j = 0$, $\langle \delta p_j^2, p_j \rangle \le 0$. Then as in case (1) we have $(\nabla \delta u^1)_j - (\nabla \delta u^2)_j = 0$.
  (3b) Consider $(\nabla \delta u^1)_j = c_1 p_j$ $(c_1 \ge 0)$, $\langle \delta p_j^1, p_j \rangle = 0$ as well as $(\nabla \delta u^2)_j = c_2 p_j$ $(c_2 \ge 0)$, $\langle \delta p_j^2, p_j \rangle = 0$. Then $\langle (\nabla \delta u^1)_j - (\nabla \delta u^2)_j, \delta p_j^1 - \delta p_j^2 \rangle = (c_1 - c_2)\langle p_j, \delta p_j^1 - \delta p_j^2 \rangle = 0$.

(3c) Consider $(\nabla \delta u^1)_j = 0$, $\langle \delta p_j^1, p_j \rangle \le 0$ and $(\nabla \delta u^2)_j = cp_j$ $(c \ge 0)$, $\langle \delta p_j^2, p_j \rangle$ $= 0$. Then we have $\langle (\nabla \delta u^1)_j - (\nabla \delta u^2)_j, \delta p_j^1 - \delta p_j^2 \rangle = \langle -cp_j, \delta p_j^1 - \delta p_j^2 \rangle \ge 0$. The analogous conclusion holds true if we interchange the upper indices ^{1} and ^{2}.

Altogether, our claim is proven. Moreover, since $D_u F(u,h)$ is strictly positive definite, we arrive at $\delta u^1 = \delta u^2$.

Thus, the equality holds in (14) with both sides being singletons, which concludes the proof. $\qquad\square$

Thus, it has been asserted that the solution mapping $S : h \mapsto u(h)$ for the lower-level problem is *B(ouligand)-differentiable* [44], i.e. locally Lipschitz continuous and directionally differentiable, everywhere on Q_h such that, with $\delta u(h; \delta h) = S'(h; \delta h)$, we have

$$u(h + \delta h) = u(h) + \delta u(h; \delta h) + o(\|\delta h\|) \quad \text{as } \delta h \to 0.$$

Furthermore, according to the chain rule, the reduced objective $\widehat{J} : h \to \mathbb{R}$ is also B-differentiable such that
(15)
$$\widehat{J}(h + \delta h) = J(u(h), h) + D_h J(u(h), h)\delta h + D_u J(u(h), h)\delta u(h; \delta h) + o(\|\delta h\|) \quad \text{as } \delta h \to 0.$$

4. **Stationarity conditions for bilevel optimization.** Our bilevel optimization problem (6) is a special instance of a mathematical program with equilibrium constraints (MPEC). The derivation of appropriate stationarity conditions is a persistent challenge for MPECs; see [38, 41] for more backgrounds on MPECs. Very often, the commonly used constraint qualifications like linear independence constraint qualification (LICQ) or Mangasarian-Fromovitz constraint qualification (MFCQ) are violated for MPECs [52], and therefore a theoretically sharp and computationally amenable characterization of the variational geometry (such as tangent and normal cones) of the solution set induced by the lower-level problem becomes a major challenge. Depending on the viewpoint (primal versus primal-dual) and the utilized generalized derivative concept, different stationarity characterizations for MPECs may arise. In this vein, various stationarity concepts are introduced in [47] when the lower-level problems are so-called complementarity problems. Whenever *strict complementarity* holds true for an MPEC, all stationarity conditions reduce to the classical KKT condition. In particular, the effect of strict complementarity in our context is discussed at the end of this section. The aforementioned stationarity concepts have been further developed and extended during the past decade; see, e.g., [38, 41, 39, 47, 51, 24, 27]. This research field still remains active in its own right.

In our context of the bilevel optimization problem (6), it is straightforward to deduce from the expansion formula (15) that

(16) $\qquad D_h J(u(h), h)\delta h + D_u J(u(h), h)\delta u(h; \delta h) \ge 0 \quad \forall \delta h \in T_{Q_h}(h)$

must hold at any local minimizer $(h, u(h))$ for (6). In fact, condition (16) is referred to as B(ouligand)-stationarity; see [38]. However, such "primal" stationarity is difficult to realize numerically, since the mapping $\delta h \mapsto \delta u(h; \delta h)$ need not be linear. For this reason, we are motivated to search for stationarity conditions in "primal-dual" form, as they typically appear in the classical KKT conditions for constrained optimization. Based on the strong regularity condition proven in Theorem 3.1 above and the Mordukhovich calculus (see the two-volume monograph [39] for reference),

we shall derive the M(ordukhovich)-stationarity for (6) in Theorem 4.2. There the *Mordukhovich (or limiting) normal cone* of $\operatorname{gph} G$ will appear in the stationarity condition, which is defined as follows.

Definition 4.1 (Mordukhovich normal cone). The Mordukhovich normal cone of a subset Q in $\mathbb{R}^{|\Omega_u|}$ at $u \in Q$, denoted by $N_Q^{(\mathrm{M})}(u)$, is defined by

$$(17) \qquad N_Q^{(\mathrm{M})}(u) = \{w \in \mathbb{R}^{|\Omega_u|} : w^k \to w, \ u^k \to u, \ w^k \in N_Q(u^k) \ \forall k\}.$$

In particular, one has $N_Q^{(\mathrm{M})}(\cdot) = N_Q(\cdot)$ whenever Q is convex. Following (10) and (11), the Mordukhovich normal cone of $\operatorname{gph} G$ can be calculated as:

$$(18) \quad N_{\operatorname{gph} G}^{(\mathrm{M})}(u, \alpha\nabla^\top p) = \Big\{ (\alpha\nabla^\top w, -v) : w \in (\mathbb{R}^{|\Omega_u|})^2 \text{ and } v \in \mathbb{R}^{|\Omega_u|} \text{ satisfy}$$

$$\exists \xi_j \in \mathbb{R}^2 : w_j = \xi_j - \langle \xi_j, p_j \rangle p_j, \ (\nabla v)_j = |(\nabla u)_j| \xi_j, \quad \text{if } (\nabla u)_j \neq 0;$$

$$w_j \in \mathbb{R}^2, \ (\nabla v)_j = 0, \quad \text{if } |p_j| < 1;$$

$$\Big(w_j \in \mathbb{R}^2, \ (\nabla v)_j = 0\Big) \vee \Big(\exists c \in \mathbb{R} : \langle w_j, p_j \rangle = 0, \ (\nabla v)_j = cp_j\Big)$$

$$\vee \Big(\exists c \leq 0 : \langle w_j, p_j \rangle \leq 0, \ (\nabla v)_j = cp_j\Big), \quad \text{if } (\nabla u)_j = 0, \ |p_j| = 1\Big\}.$$

We are now ready to present the M-stationarity condition for (6). Given that the strong regularity condition is satisfied at any feasible solution (u, h, p) as justified in Theorem 3.1, M-stationarity of a local minimizer for (6) follows as a direct consequence of Theorem 3.1 and Proposition 3.2 in [42]. The proof for this result in [42] used the strong regularity condition as a proper constraint qualification.

Theorem 4.2 (M-stationarity). *Let $(u, h, p) \in \mathbb{R}^{|\Omega_u|} \times Q_h \times Q_p$ be any feasible point satisfying (8). If (u, h) is a local minimizer for the bilevel optimization problem (6), then the following M-stationarity condition must hold true for some $(w, v) \in \big(\mathbb{R}^{|\Omega_u|}\big)^2 \times \mathbb{R}^{|\Omega_u|}$:*

$$(19) \qquad \begin{cases} D_u J(u,h)^\top + \alpha\nabla^\top w + D_u F(u,h)^\top v = 0, \\ 0 \in D_h J(u,h)^\top + D_h F(u,h)^\top v + N_{Q_h}(h), \\ (\alpha\nabla^\top w, -v) \in N_{\operatorname{gph} G}^{(\mathrm{M})}(u, \alpha\nabla^\top p), \end{cases}$$

where $N_{\operatorname{gph} G}^{(\mathrm{M})}$ is the Mordukhovich normal cone of $\operatorname{gph} G$ given in (18).

Though theoretically sharp, the M-stationarity condition in the above theorem is in general not guaranteed by numerical algorithms. Instead, we resort to a Clarke-type stationarity, termed C-stationarity in the following corollary. The C-stationarity is slightly weaker than the M-stationarity due to the relation $N_{\operatorname{gph} G}^{(\mathrm{M})}(u, \alpha\nabla^\top p) \subset N_{\operatorname{gph} G}^{(\mathrm{C})}(u, \alpha\nabla^\top p)$, but can be guaranteed by a projected-gradient-type algorithm proposed in section 5 below.

Corollary 4.3 (C-stationarity). *Let $(u, h, p) \in \mathbb{R}^{|\Omega_u|} \times Q_h \times Q_p$ be any feasible point satisfying (8). If (u, h) is a local minimizer for the bilevel optimization problem (6), the following C-stationarity condition must hold true for some $(w, v) \in \big(\mathbb{R}^{|\Omega_u|}\big)^2 \times \mathbb{R}^{|\Omega_u|}$:*

$$(20) \qquad \begin{cases} D_u J(u,h)^\top + \alpha\nabla^\top w + D_u F(u,h)^\top v = 0, \\ 0 \in D_h J(u,h)^\top + D_h F(u,h)^\top v + N_{Q_h}(h), \\ (\alpha\nabla^\top w, -v) \in N_{\operatorname{gph} G}^{(\mathrm{C})}(u, \alpha\nabla^\top p), \end{cases}$$

where

$$(21) \quad N_{\mathrm{gph}\,G}^{(\mathrm{C})}(u, \alpha\nabla^\top p) = \Big\{ (\alpha\nabla^\top w, -v) : w \in (\mathbb{R}^{|\Omega_u|})^2 \text{ and } v \in \mathbb{R}^{|\Omega_u|} \text{ satisfy that}$$

$$\exists \xi_j \in \mathbb{R}^2 : w_j = \xi_j - \langle \xi_j, p_j \rangle p_j, \ (\nabla v)_j = |(\nabla u)_j| \xi_j, \quad \text{if } (\nabla u)_j \neq 0;$$

$$w_j \in \mathbb{R}^2, \ (\nabla v)_j = 0, \quad \text{if } |p_j| < 1;$$

$$\exists c \in \mathbb{R} : (\nabla v)_j = c p_j, \ \langle w_j, (\nabla v)_j \rangle \geq 0, \quad \text{if } (\nabla u)_j = 0, \ |p_j| = 1 \Big\}.$$

We say that *strict complementarity* holds at a feasible point (u, h, p) whenever the biactive set is empty, i.e.

$$(22) \qquad\qquad \{j \in \Omega_u : (\nabla u)_j = 0, \ |p_j| = 1\} = \emptyset.$$

Under strict complementarity, one immediately observes the equivalence of M- and C-stationarity as $N_{\mathrm{gph}\,G}^{(\mathrm{M})}(u, \alpha\nabla^\top p) = N_{\mathrm{gph}\,G}^{(\mathrm{C})}(u, \alpha\nabla^\top p)$. The scenarios of strict complementarity are studied in detail in section 5.1, where it will become evident to the reader that all B-, M-, and C-stationarity concepts are equivalent under strict complementarity; see Corollary 5.3.

5. **Hybrid projected gradient method.** This section is devoted to the development and the convergence analysis of a hybrid projected gradient algorithm to compute a C-stationary point for the bilevel optimization problem (6). Most existing numerical solvers for MPECs adopt regularization/smoothing/relaxation on the complementary structure in the lower-level problem, see e.g. [21, 48, 19], even though the complementary structure induced by (8) is more involved than those in the previous works due to the presence of nonlinearity. Motivated by the recent work in [27], here we devise an algorithm which avoids redundant regularization, e.g., when the current iterate is a continuously differentiable point for the reduced objective $\widehat{J}$.

5.1. **Differentiability given strict complementarity.** In this subsection, we assume that strict complementarity, i.e. condition (22), holds at a feasible point (u, h, p). In this scenario, the sensitivity equation (12) is fully characterized by the following linear system:

$$(23) \qquad \begin{bmatrix} D_u F(u, h) & \alpha\nabla^\top \\ (-I + pp^\top)\nabla & \mathrm{diag}(|\nabla u|e) \end{bmatrix} \begin{bmatrix} \delta u \\ \delta p \end{bmatrix} = \begin{bmatrix} -D_h F(u, h)\delta h \\ 0 \end{bmatrix}.$$

Here e is the identity vector in $(\mathbb{R}^{|\Omega|})^2$, i.e. $e_j = (1, 1)$ for all $j \in \Omega_u$, and $\mathrm{diag}(|\nabla u|e)$ denotes a diagonal matrix with its diagonal elements given by the vector $|\nabla u|e$. As a special case in Theorem 3.4, for any given $\delta h \in T_{Q_h}(h)$, the linear system (23) always admits a solution $(\delta u, \delta p)$ which is unique in δu. Thus, the differential mapping $\frac{\delta u}{\delta h}(h) : \delta h \mapsto \delta u$ defined by equation (23) is a continuous linear mapping, and therefore the reduced objective $\widehat{J}$ in (7) is continuously differentiable at h. On the other hand, the adjoint of the differential $\frac{\delta u}{\delta h}(h)$, denoted by $\frac{\delta u}{\delta h}(h)^\top$, is required when computing $D_h \widehat{J}(h)$. This will be addressed through the adjoint equation in Theorem 5.2 below.

Lemma 5.1. *Assume that (u, h, p) is a feasible point satisfying (8) and strict complementarity holds at (u, h, p). Let $\Pi_{\delta u}$ be a canonical projection such that $\Pi_{\delta u}(\delta u, \delta p) = (\delta u, 0)$ for all $(\delta u, \delta p) \in \mathbb{R}^{|\Omega_u|} \times (\mathbb{R}^{|\Omega_u|})^2$. Then the following relations hold true:*

(i) $\mathrm{Ker} \begin{bmatrix} D_u F(u,h)^\top & \nabla^\top(-I + pp^\top) \\ \alpha\nabla & \mathrm{diag}(|\nabla u|e) \end{bmatrix} \subset \mathrm{Ker}\,\Pi_{\delta u}$.

(ii) $\mathrm{Ran}\,\Pi_{\delta u} \subset \mathrm{Ran} \begin{bmatrix} D_u F(u,h)^\top & \nabla^\top(-I + pp^\top) \\ \alpha\nabla & \mathrm{diag}(|\nabla u|e) \end{bmatrix}$.

Proof. We first prove (i). For this purpose, let

$$\begin{bmatrix} D_u F(u,h)^\top & \nabla^\top(-I + pp^\top) \\ \alpha\nabla & \mathrm{diag}(|\nabla u|e) \end{bmatrix} \begin{bmatrix} v \\ \eta \end{bmatrix} = \begin{bmatrix} 0 \\ 0 \end{bmatrix},$$

which implies

$$0 = \langle v, D_u F(u,h)^\top v \rangle + \langle \nabla v, (-I + pp^\top)\eta \rangle$$

$$= \langle v, D_u F(u,h)^\top v \rangle + \frac{1}{\alpha}\langle |\nabla u|\eta, (I - pp^\top)\eta \rangle$$

$$= \langle v, D_u F(u,h)^\top v \rangle + \frac{1}{\alpha} \sum_{j \in \Omega_u} |(\nabla u)_j|(|\eta_j|^2 - |\langle p_j, \eta_j \rangle|^2).$$

Owing to the strict positive definiteness of $D_u F(u,h)$ as well as the non-negativity of the second term in the above equation, we verify that $v = 0$.

To justify (ii), in view of the fundamental theorem of linear algebra, it suffices to prove

$$\mathrm{Ker} \begin{bmatrix} D_u F(u,h) & \alpha\nabla^\top \\ (-I + pp^\top)\nabla & \mathrm{diag}(|\nabla u|e) \end{bmatrix} \subset \mathrm{Ker}\,\Pi_{\delta u}.$$

For this purpose, consider

(24) $$\begin{bmatrix} D_u F(u,h) & \alpha\nabla^\top \\ (-I + pp^\top)\nabla & \mathrm{diag}(|\nabla u|e) \end{bmatrix} \begin{bmatrix} \delta u \\ \delta p \end{bmatrix} = \begin{bmatrix} 0 \\ 0 \end{bmatrix}.$$

Then we have

(25) $$\langle \delta u, D_u F(u,h)\delta u \rangle + \alpha\langle \delta p, pp^\top\nabla\delta u \rangle + \alpha\langle \delta p, |\nabla u|\delta p \rangle = 0.$$

Due to strict complementarity, only two possible scenarios may occur. If $(\nabla u)_j \neq 0$, then the second row of equation (24) yields $\delta p_j = \frac{1}{|(\nabla u)_j|}(I - p_j p_j^\top)(\nabla\delta u)_j$, and thus $\langle \delta p_j, p_j p_j^\top(\nabla\delta u)_j \rangle \geq 0$. If $|p_j| < 1$, then $(\nabla u)_j = 0$ and $0 = |(I - p_j p_j^\top)(\nabla\delta u)_j| \geq (1 - |p_j|^2)|(\nabla\delta u)_j|$, which implies $\langle \delta p_j, p_j p_j^\top(\nabla\delta u)_j \rangle = 0$. Altogether, we have shown $\langle \delta p, pp^\top\nabla\delta u \rangle \geq 0$. Moreover, since the third term in (25) is also non-negative and $D_u F(u,h) = -\mu\Delta + K(h)^\top K(h)$ is strictly positive definite, we must have $\delta u = 0$. Thus, (ii) is proven. $\square$

Theorem 5.2. *As in Lemma 5.1, assume that (u,h,p) is a feasible point satisfying (8) and strict complementarity holds at (u,h,p). Then $\frac{\delta u}{\delta h}(h)^\top$ is a linear mapping such that $\frac{\delta u}{\delta h}(h)^\top : \zeta \mapsto D_h F(u,h)^\top v$ with $(\zeta, v, \eta) \in \mathbb{R}^{|\Omega_u|} \times \mathbb{R}^{|\Omega_u|} \times (\mathbb{R}^{|\Omega_u|})^2$ satisfying the following adjoint equation:*

(26) $$\begin{bmatrix} D_u F(u,h)^\top & \nabla^\top(-I + pp^\top) \\ \alpha\nabla & \mathrm{diag}(|\nabla u|e) \end{bmatrix} \begin{bmatrix} v \\ \eta \end{bmatrix} = \begin{bmatrix} -\zeta \\ 0 \end{bmatrix}.$$

Proof. It follows from Lemma 5.1 that $\zeta \mapsto v$ is a continuous linear mapping and, therefore, so is $\frac{\delta u}{\delta h}(h)^\top$. To show the adjoint relation between $\frac{\delta u}{\delta h}(h)$ and $\frac{\delta u}{\delta h}(h)^\top$, consider an arbitrary pair $(\delta u, \delta h, \delta p)$ which satisfies (23), i.e. $\delta u = \frac{\delta u}{\delta h}(h)\delta h$, and (ζ, v, η) which satisfies (26). Then we derive that

$$\left\langle \zeta, \frac{\delta u}{\delta h}(h)\delta h \right\rangle = -\left\langle \begin{bmatrix} \delta u \\ \delta p \end{bmatrix}, \begin{bmatrix} D_u F(u,h)^\top & \nabla^\top(-I + pp^\top) \\ \alpha\nabla & \mathrm{diag}(|\nabla u|e) \end{bmatrix} \begin{bmatrix} v \\ \eta \end{bmatrix} \right\rangle$$

$$= -\left\langle \begin{bmatrix} D_u F(u,h) & \alpha \nabla^\top \\ (-I + pp^\top)\nabla & \operatorname{diag}(|\nabla u|e) \end{bmatrix} \begin{bmatrix} \delta u \\ \delta p \end{bmatrix}, \begin{bmatrix} v \\ \eta \end{bmatrix} \right\rangle$$

$$= \langle v, D_h F(u,h)\delta h \rangle = \langle D_h F(u,h)^\top v, \delta h \rangle = \left\langle \frac{\delta u}{\delta h}(h)^\top \zeta, \delta h \right\rangle,$$

which concludes the proof. $\qquad\square$

As a consequence of Theorem 5.2, at a feasible point (u, h, p) where strict complementarity holds, the gradient of the reduced objective can be calculated as

$$(27) \quad D_h \widehat{J}(h)^\top = D_h J(u,h)^\top + \frac{\delta u}{\delta h}(h)^\top D_u J(u,h)^\top = D_h J(u,h)^\top + D_h F(u,h)^\top v,$$

where (v, η) satisfies the adjoint equation (26) with $\zeta = D_u J(u,h)^\top$. For numerical purposes, we note that the adjoint equation (26) can be solved iteratively by, e.g., the quasi-minimal residual method [20]. For the sake of our convergence analysis in section 5.3, we also introduce an auxiliary variable w defined by

$$(28) \qquad\qquad w := \frac{1}{\alpha}(-I + p(p)^\top)\eta,$$

which parallels the auxiliary variable w^γ later in (38) for the smoothing case. To conclude section 5.1, we point out that one can readily deduce from (27) the equivalence among the B-, M-, and C-stationarity under strict complementarity.

Corollary 5.3 (Stationarity under strict complementarity). *If strict complementarity holds at a feasible point (u, h, p), then B-stationarity (16), M-stationarity (19), and C-stationarity (20) are all equivalent.*

5.2. **Local smoothing at a non-differentiable point.** The solution mapping $h \mapsto u$ for the lower-problem in (6) is only B-differentiable (rather than continuously differentiable) at a feasible point (u, h, p) where the biactive set $\{j \in \Omega_u : (\nabla u)_j = 0, \ |p_j| = 1\}$ is nonempty. In this scenario, continuous optimization techniques are not directly applicable. Instead, we utilize a local smoothing approach by replacing the Lipschitz continuous function $\| \cdot \|_1$ in (2) by a C^2-approximation $\| \cdot \|_{1,\gamma} : \left(\mathbb{R}^{|\Omega_u|}\right)^2 \to \mathbb{R}$, which is defined for each $\gamma > 0$ by $\|p\|_{1,\gamma} := \sum_{j \in \Omega_u} \varphi_\gamma(p_j)$ with

$$(29) \qquad\qquad \varphi_\gamma(s) = \begin{cases} -\frac{1}{8\gamma^3}|s|^4 + \frac{3}{4\gamma}|s|^2 & \text{if } |s| < \gamma, \\ |s| - \frac{3\gamma}{8} & \text{if } |s| \geq \gamma. \end{cases}$$

The first-order and second-order derivatives of φ_γ can be calculated as

$$(30) \qquad\qquad \varphi_\gamma'(s) = \begin{cases} (\frac{3}{2\gamma} - \frac{1}{2\gamma^3}|s|^2)s & \text{if } |s| < \gamma, \\ \frac{1}{|s|}s & \text{if } |s| \geq \gamma. \end{cases}$$

and

$$(31) \qquad\qquad \varphi''(s) = \begin{cases} (\frac{3}{2\gamma} - \frac{1}{2\gamma^3}|s|^2)I_{\mathbb{R}^2} - \frac{1}{\gamma^3}ss^\top & \text{if } |s| < \gamma, \\ \frac{1}{|s|}I_{\mathbb{R}^2} - \frac{1}{|s|^3}ss^\top & \text{if } |s| \geq \gamma. \end{cases}$$

We remark that the same smoothing function was used in [35] for parameter learning, but other choices are possible as well.

The resulting smoothed bilevel optimization problem appears as

$$(32) \quad \begin{aligned} &\min && J(u^\gamma, h) \\ &\text{s.t.} && u^\gamma = \arg\min_u \frac{\mu}{2}\|\nabla u\|^2 + \frac{1}{2}\|K(h)u - z\|^2 + \alpha\|\nabla u\|_{1,\gamma}, \\ & && u^\gamma \in \mathbb{R}^{|\Omega_u|}, \ h \in Q_h. \end{aligned}$$

The corresponding Euler-Lagrange equation for the lower-level problem in (32) is given by

$$(33) \qquad r(u^\gamma; h, \gamma) := (-\mu\Delta + K(h)^\top K(h))u^\gamma - K(h)^\top z + \alpha\nabla^\top(\varphi'_\gamma(\nabla u^\gamma)) = 0,$$

which induces a continuously differentiable mapping $h \mapsto u^\gamma(h)$ according to the (classical) implicit function theorem. Moreover, the sensitivity equation for (33) is given by

$$(34) \qquad \left(D_u F(u^\gamma, h) + \alpha\nabla^\top\varphi''_\gamma(\nabla u^\gamma)\nabla\right) D_h u^\gamma(h) = -D_h F(u^\gamma, h).$$

Analogous to (7), we may also reformulate the smoothed bilevel problem (32) in the reduced form as

$$(35) \qquad \begin{aligned} \min \quad & \breve{J}_\gamma(h) := J(u^\gamma(h), h) \\ \text{s.t.} \quad & h \in Q_h. \end{aligned}$$

The gradient of $\breve{J}_\gamma$ can be calculated as

$$(36) \qquad D_h\breve{J}_\gamma(h)^\top = D_h J(u^\gamma, h)^\top + D_h F(u^\gamma, h)^\top v^\gamma,$$

where v^γ satisfies the adjoint equation

$$(37) \qquad \left(D_u F(u^\gamma, h)^\top + \alpha\nabla^\top\varphi''_\gamma(\nabla u^\gamma)\nabla\right) v^\gamma = -D_u J(u^\gamma, h)^\top.$$

Thus, any stationary point (u^γ, h) of the smoothed bilevel optimization problem (32) must satisfy the following stationarity condition

$$(38) \qquad \begin{cases} F(u^\gamma, h) + \alpha\nabla^\top p^\gamma = 0, \\ p^\gamma = \varphi'_\gamma(\nabla u^\gamma), \\ D_u F(u^\gamma, h)^\top v^\gamma + \alpha\nabla^\top w^\gamma = -D_u J(u^\gamma, h)^\top, \\ w^\gamma = \varphi''_\gamma(\nabla u^\gamma)\nabla v^\gamma, \\ 0 \in D_h J(u^\gamma, h)^\top + D_h F(u^\gamma, h)^\top v^\gamma + N_{Q_h}(h), \end{cases}$$

for some $p^\gamma \in \left(\mathbb{R}^{|\Omega_u|}\right)^2$, $w^\gamma \in \left(\mathbb{R}^{|\Omega_u|}\right)^2$, and $v^\gamma \in \mathbb{R}^{|\Omega_u|}$.

We remark that finding a stationary point of the (smooth) constrained minimization problem (35) can be accomplished by standard optimization algorithms; see [40]. As a subroutine in Algorithm 5.5 below, we adopt a simple projected gradient method whose convergence analysis can be found in [22]. The following theorem establishes the consistency on how a stationary point of the smoothed bilevel problem (32) approaches a C-stationary point of the original bilevel problem (6) as γ vanishes.

Theorem 5.4 (Consistency of smoothing). *Let $\{\gamma^k\}$ be any sequence of positive scalars such that $\gamma^k \to 0^+$. For each γ^k, let $(u^k, h^k) \in \mathbb{R}^{|\Omega_u|} \times Q_h$ be a stationary point of (32) such that condition (38) holds for some $(p^k, w^k, v^k) \in \left(\mathbb{R}^{|\Omega_u|}\right)^2 \times \left(\mathbb{R}^{|\Omega_u|}\right)^2 \times \mathbb{R}^{|\Omega_u|}$. Then any accumulation point of $\{(u^k, h^k, p^k, w^k, v^k)\}$ is a feasible C-stationary point for (6) satisfying (8) and (20).*

Proof. Let $(u^*, h^*, p^*, w^*, v^*)$ be an arbitrary accumulation point of $\{(u^k, h^k, p^k, w^k, v^k)\}$. Then the first condition in (8) and the first condition in (20) immediately follow from continuity. The second condition in (20) also follows due to the closedness of the normal cone mapping $N_{Q_h}(\cdot)$; see, e.g., Proposition 6.6 in [45].

For those $j \in \Omega_u$ where $(\nabla u^*)_j \neq 0$, we have for all sufficiently large k that $p^k_j = \frac{(\nabla u^k)_j}{|(\nabla u^k)_j|}$, and therefore $p^*_j = \frac{(\nabla u^*)_j}{|(\nabla u^*)_j|}$. On the other hand, $p^*_j \in Q_p$ clearly holds if $(\nabla u^*)_j = 0$. Altogether, the feasibility of (u^*, h^*, p^*) is verified.

It remains to show $(\alpha\nabla^\top w^*, -v^*) \in N^{(\mathrm{C})}_{\mathrm{gph}\,G}(u^*, \alpha\nabla^\top p^*)$, for which the proof is divided into three cases as follows.

(1) If $(\nabla u^*)_j \neq 0$, then we have for all sufficiently large k that $|(\nabla u^k)_j| \geq \gamma^k$ and therefore

$$w^k_j = \frac{1}{|(\nabla u^k)_j|}(\nabla v^k)_j - \frac{1}{|(\nabla u^k)_j|}\langle(\nabla v^k)_j, p^k_j\rangle p^k_j.$$

Passing $k \to \infty$, the first condition in (21) is fulfilled with $\xi_j = \frac{1}{|(\nabla u^*)_j|}(\nabla v^*)_j$.

(2) If $|p^*_j| < 1$, then we have for all sufficiently large k that $|p^k_j| < 1$ and, therefore, $|(\nabla u^k)_j| < \gamma^k$. This implies $(\nabla u^*)_j = 0$. Let $q_j \in \mathbb{R}^2$ be an arbitrary accumulation point of the uniformly bounded sequence $\{(\nabla u^k)_j/\gamma^k\}$. We obviously have $|q_j| \leq 1$. Then it follows from $p^k = \varphi'_{\gamma^k}(\nabla u^k)$ that $p^*_j = (3/2 - |q_j|^2/2)q_j$. Since $|p^*_j| < 1$, we must have $|q_j| < 1$. Since $w^k = \varphi''_{\gamma^k}(\nabla u^k)\nabla v^k$, we have

$$\gamma^k w^k_j = \left(\frac{3}{2} - \frac{|(\nabla u^k)_j|^2}{2(\gamma^k)^2}\right)(\nabla v^k)_j - \left\langle(\nabla v^k)_j, \frac{(\nabla u^k)_j}{\gamma^k}\right\rangle\frac{(\nabla u^k)_j}{\gamma^k}.$$

Passing $k \to \infty$, we obtain

$$\frac{3 - |q_j|^2}{2}(\nabla v^*)_j - \langle q_j, (\nabla v^*)_j\rangle q_j = 0,$$

which indicates that $(\nabla v^*)_j = cq_j$ for some $c \in \mathbb{R}$. Thus it follows that $\frac{3}{2}(1 - |q_j|^2)(\nabla v^*)_j = 0$, and thus $(\nabla v^*)_j = 0$ as requested by the second condition in (21).

(3) Now we investigate the third condition in (21) where $(\nabla u^*)_j = 0$ and $|p^*_j| = 1$ under the following two circumstances.

(3a) There exists an infinite index subset $\{k'\} \subset \{k\}$ such that $(\nabla u^{k'})_j \geq \gamma^{k'}$ for all k'. Then it holds for all k' that

$$(39) \qquad \begin{cases} |p^{k'}_j| = 1, \\ w^{k'}_j = \dfrac{1}{|(\nabla u^{k'})_j|}(\nabla v^{k'})_j - \dfrac{1}{|(\nabla u^{k'})_j|}\langle(\nabla v^{k'})_j, p^{k'}_j\rangle p^{k'}_j, \end{cases}$$

and therefore

$$\begin{cases} \langle w^{k'}_j, p^{k'}_j\rangle = 0, \\ |(\nabla u^{k'})_j| w^{k'}_j = (\nabla v^{k'})_j - \langle(\nabla v^{k'})_j, p^{k'}_j\rangle p^{k'}_j. \end{cases}$$

Passing $k' \to \infty$, we have $\langle w^*_j, p^*_j\rangle = 0$ and $(\nabla v^*)_j - \langle(\nabla v^*)_j, p^*_j\rangle p^*_j = 0$. Thus the third condition in (21) is fulfilled.

(3b) There exists an infinite index subset $\{k'\} \subset \{k\}$ such that $(\nabla u^{k'})_j < \gamma^{k'}$ for all k'. Then analogous to case (2), we have for all k' that

$$(40) \qquad \begin{cases} p^{k'}_j = \left(\dfrac{3}{2\gamma^{k'}} - \dfrac{|\nabla u^{k'}_j|^2}{2(\gamma^{k'})^3}\right)\nabla u^{k'}_j, \\ \gamma^{k'} w^{k'}_j = \left(\dfrac{3}{2} - \dfrac{|(\nabla u^{k'})_j|^2}{2(\gamma^{k'})^2}\right)(\nabla v^{k'})_j - \left\langle(\nabla v^{k'})_j, \dfrac{(\nabla u^{k'})_j}{\gamma^{k'}}\right\rangle\dfrac{(\nabla u^{k'})_j}{\gamma^{k'}}. \end{cases}$$

Let $q_j \in \mathbb{R}^2$ be an arbitrary accumulation point of the uniformly bounded sequence $\{(\nabla u^{k'})_j/\gamma^{k'}\}$. Then we have $p^*_j = (\frac{3}{2} - \frac{1}{2}|q_j|^2)q_j$. It follows from $|p^*_j| = 1$ that $|q_j| = 1$ must hold. Since this holds true for an arbitrary accumulation point q_j, we infer that $\lim_{k'\to\infty}(\nabla u^{k'})_j/\gamma^k = p^*_j$ and

further from the second equation in (40) that $(\nabla v^*)_j - \langle (\nabla v^*)_j, p_j^* \rangle p_j^* = 0$, i.e. $(\nabla v^*)_j = cp_j^*$ for some $c \in \mathbb{R}$. On the other hand, equation (40) also yields that

$$\langle w_j^{k'}, (\nabla v^{k'})_j \rangle = \left(\frac{3}{2\gamma^{k'}} - \frac{|(\nabla u^{k'})_j|^2}{2(\gamma^{k'})^3} \right) |(\nabla v^{k'})_j|^2 - \frac{1}{\gamma^{k'}} \left| \left\langle (\nabla v^{k'})_j, \frac{(\nabla u^{k'})_j}{\gamma^{k'}} \right\rangle \right|^2$$

$$\geq \frac{3}{2\gamma^{k'}} \left(1 - \left| \frac{(\nabla u^{k'})_j}{\gamma^{k'}} \right|^2 \right) |(\nabla v^{k'})_j|^2 \geq 0.$$

Passing $k' \to \infty$, the third condition in (21) is again fulfilled.

$\square$

5.3. **Hybrid projected gradient method.** Now we present in Algorithm 5.5 a hybrid projected gradient method for finding a C-stationary point of the bilevel optimization problem (6). In this algorithm, at a feasible point (u^k, h^k, p^k) where strict complementarity holds, we calculate $D_h \widehat{J}(h^k)^\top$ according to formula (27) and perform a projected gradient step by setting

$$(41) \qquad \widehat{h}^k(\tau^k) := P_{Q_h}[h^k - \tau^k D_h \widehat{J}(h^k)^\top]$$

for some proper step size $\tau^k > 0$; see steps 6–15 of Algorithm 5.5. If strict complementarity is violated at (u^k, h^k, p^k), we rather perform a projected gradient step on the smoothed bilevel problem (32) with $\gamma = \gamma^k > 0$, i.e.

$$(42) \qquad \breve{h}^k(\tau^k) := P_{Q_h}[h^k - \tau^k D_h \breve{J}_{\gamma^k}(h^k)^\top];$$

see steps 16–25. Moreover, the method takes precautions against the critical case where the step size τ^k in (41) tends to zero along the iterations. This case may possibly occur when the $\{(u^k, h^k, p^k)\}$ converges to some $\{(u^*, h^*, p^*)\}$ where strict complementarity fails, even if strict complementarity holds for each feasible point (u^k, h^k, p^k) along the sequence. In such a critical case, we also resort to the smoothed bilevel problem as in (42); see steps 11–13. The overall hybrid algorithm is detailed below.

Algorithm 5.5 (Hybrid projected gradient method)**.**
Require: inputs $\alpha > 0$, $0 \leq \mu \ll \alpha$, $0 < \underline{\tau} \ll \bar{\tau}$, $0 < \sigma_J < 1$, $0 < \rho_\tau < 1$,
 $0 < \rho_\gamma < 1$, $\sigma_h > 0$, $\mathrm{tol}_h > 0$, $\mathrm{tol}_\gamma > 0$.
 1: Initialize $\gamma^1 > 0$, a feasible point $(u^1, h^1, p^1) \in \mathbb{R}^{|\Omega_u|} \times Q_h \times \left(\mathbb{R}^{|\Omega_u|} \right)^2$ satisfying
  (8), $\widetilde{u}^1 := u^1$, $\widetilde{p}^1 := p^1$, $\mathcal{I} := \{1\}$, and $k := 1$.
 2: **loop**
 3:   **if** strict complementarity condition (22) is violated at $(\widetilde{u}^k, h^k, \widetilde{p}^k)$ (i.e. the
   biactive set $\{j \in \Omega_u : (\nabla \widetilde{u}^k)_j = 0, \ |\widetilde{p}_j^k| = 1\}$ is nonempty) **or** $J(\widetilde{u}^k, h^k) >$
   $J(u^{\max(\mathcal{I})}, h^{\max(\mathcal{I})})$ **then**
 4:    Go to step 16.
 5:   **end if**
 6:   Set $u^k := \widetilde{u}^k$, $p^k := \widetilde{p}^k$. Compute $D_h \widehat{J}(h^k)^\top$ using formula (27). Define the
   mapping $\widehat{h}^k(\cdot)$ by (41).
 7:   **if** $\|\widehat{h}^k(\bar{\tau}) - h^k\| \leq \mathrm{tol}_h$ **then**
 8:    Return (u^k, h^k) as a C-stationary point of (6) and terminate the algorithm.
 9:   **end if**

10:     Perform the backtracking line search on $\widehat{h}^k(\cdot)$, i.e. find τ^k as the largest element in $\{\bar{\tau}(\rho_\tau)^l : l = 0, 1, 2, ...\}$ such that $\widehat{h}^k(\tau^k)$ fulfills the following Armijo-type condition:

(43) $$\widehat{J}(\widehat{h}^k(\tau^k)) \leq \widehat{J}(h^k) + \sigma_J D_h \widehat{J}(h^k)(\widehat{h}^k(\tau^k) - h^k).$$

11:     **if** $\tau^k < \underline{\tau}$ **then**
12:         Go to step 16.
13:     **end if**
14:     Set $h^{k+1} := \widehat{h}^k(\tau^k)$ and $\mathcal{I} := \mathcal{I} \cup \{k\}$. Generate $\widetilde{u}^{k+1} \in \mathbb{R}^{|\Omega_u|}$ and $\widetilde{p}^{k+1} \in \left(\mathbb{R}^{|\Omega_u|}\right)^2$ such that $(\widetilde{u}^{k+1}, h^{k+1}, \widetilde{p}^{k+1})$ satisfies the state equation (8).
15:     Set $\gamma^{k+1} := \gamma^k$. Go to step 26.
16:     Solve equation (33) with $(\gamma, h) = (\gamma^k, h^k)$ for $u^\gamma =: u^k$, and equation (37) with $(\gamma, u^\gamma, h) = (\gamma^k, u^k, h^k)$ for $v^\gamma =: v^k$. Then calculate $D_h \breve{J}_{\gamma^k}(h^k)^\top$ using formula (36). Define the mapping $\breve{h}^k(\cdot)$ by (42).
17:     **if** $\|\breve{h}^k(\bar{\tau}) - h^k\| \leq \sigma_h \gamma^k$ **then**
18:         **if** $\gamma^k = \mathrm{tol}_\gamma$ **then**
19:             Return (u^k, h^k) as a C-stationary point of (6) and terminate the algorithm.
20:         **else**
21:             Set $\gamma^{k+1} := \max(\rho_\gamma \gamma^k, \mathrm{tol}_\gamma)$ and $(\widetilde{u}^{k+1}, h^{k+1}, \widetilde{p}^{k+1}) := (\widetilde{u}^k, h^k, \widetilde{p}^k)$. Go to step 26.
22:         **end if**
23:     **end if**
24:     Perform the backtracking line search on $\breve{h}^k(\cdot)$, i.e. find τ^k as the largest element in $\{\bar{\tau}(\rho_\tau)^l : l = 0, 1, 2, ...\}$ such that $\breve{h}^k(\tau^k)$ fulfills the following Armijo-type condition:

(44) $$\breve{J}_{\gamma^k}(\breve{h}^k(\tau^k)) \leq \breve{J}_{\gamma^k}(h^k) + \sigma_J D_h \breve{J}_{\gamma^k}(h^k)(\breve{h}^k(\tau^k) - h^k).$$

25:     Set $h^{k+1} := \breve{h}^k(\tau^k)$. Generate $\widetilde{u}^{k+1} \in \mathbb{R}^{|\Omega_u|}$ and $\widetilde{p}^{k+1} \in \left(\mathbb{R}^{|\Omega_u|}\right)^2$ such that $(\widetilde{u}^{k+1}, h^{k+1}, \widetilde{p}^{k+1})$ satisfies the state equation (8). Set $\gamma^{k+1} := \gamma^k$.
26:     Set $k := k + 1$.
27: **end loop**

In the following, we prove convergence of Algorithm 5.5 towards C-stationarity. To begin with, we collect a technical result from Lemma 3 in [22], which will be used several times in our convergence analysis.

Lemma 5.6. *The mappings* $\tau^k \mapsto \|\widehat{h}^k(\tau^k) - h^k\|/\tau^k$ *and* $\tau^k \mapsto \|\breve{h}^k(\tau^k) - h^k\|/\tau^k$ *are both monotonically decreasing on* $[0, \infty)$.

Based on Lemma 5.6, it is shown in the following lemma that the backtracking line searches in Algorithm 5.5 enjoy good properties.

Lemma 5.7. *The backtracking line searches in steps 10 and 24 of Algorithm 5.5 always terminate with success after finitely many trails.*

Proof. As the line search in step 24 is performed on the continuously differentiable objective $\breve{J}_{\gamma^k}$, the proof of Proposition 2 in [22] can be directly applied.

However, this proof needs to be adapted for step 10 since it is performed on the B-differentiable objective $\widehat{J}$. In this case, we proceed with a proof by contradiction.

Assume that (43) is violated for all $\tau^k = \tau_l^k := \bar{\tau}(\rho_\tau)^l$ with $l = 0, 1, 2, ...$ Then h^k cannot be stationary, since otherwise $\widehat{h}^k(\tau^k) = h^k$ and (43) holds true for any $\tau^k > 0$.

Since $\widehat{J}$ is B-differentiable, we have

$$(45) \quad \widehat{J}(\widehat{h}^k(\tau_l^k)) - \widehat{J}(h^k) = D_h\widehat{J}(h^k)(\widehat{h}^k(\tau_l^k) - h^k) + o(\|\widehat{h}^k(\tau_l^k) - h^k\|), \quad \text{as } l \to \infty.$$

This, together with the violation of (43), gives

$$(46) \quad (1 - \sigma_J)D_h\widehat{J}(h^k)(\widehat{h}^k(\tau_l^k) - h^k) + o(\|\widehat{h}^k(\tau_l^k) - h^k\|) > 0, \quad \text{as } l \to \infty.$$

Moreover, due to the relation (41), we also have

$$(47) \quad D_h\widehat{J}(h^k)(h^k - \widehat{h}^k(\tau_l^k)) \geq \frac{\|\widehat{h}^k(\tau_l^k) - h^k\|^2}{\tau_l^k},$$

which further implies
(48)
$$o(\|\widehat{h}^k(\tau_l^k) - h^k\|) > (1 - \sigma_J)D_h\widehat{J}(h^k)(h^k - \widehat{h}^k(\tau_l^k)) \geq (1 - \sigma_J)\frac{\|\widehat{h}^k(\tau_l^k) - h^k\|^2}{\tau_l^k}, \quad \text{as } l \to \infty.$$

Thus, it follows from Lemma 5.6 that

$$(49) \quad \frac{\|\widehat{h}^k(\bar{\tau}) - h^k\|}{\bar{\tau}} \leq \frac{\|\widehat{h}^k(\tau_l^k) - h^k\|}{\tau_l^k} \to 0, \quad \text{as } l \to \infty.$$

This contradicts that h^k is not stationary.   □

For the sake of our convergence analysis, we consider $\text{tol}_h = \text{tol}_\gamma = 0$ in the remainder of this section.

Lemma 5.8. *Let the sequence $\{(u^k, h^k, p^k) : k \in \mathcal{I}\}$ be generated by Algorithm 5.5. If $|\mathcal{I}|$ is infinite, then we have*

$$(50) \quad \liminf_{k \to \infty, \ k \in \mathcal{I}} \left\| h^k - P_{Q_h}[h^k - \bar{\tau}D_h\widehat{J}(h^k)^\top] \right\| = 0.$$

Proof. We restrict ourselves to $k \in \mathcal{I}$ throughout this proof. It follows from Lemma 5.6 and the satisfaction of the Armijo-type condition (43) that

$$\widehat{J}(h^k) - \widehat{J}(h^{k+1}) = \widehat{J}(h^k) - \widehat{J}(\widehat{h}^k(\tau^k)) \geq \sigma_J D_h\widehat{J}(h^k)(h^k - \widehat{h}^k(\tau^k))$$
$$\geq \sigma_J \frac{\|h^k - \widehat{h}^k(\tau^k)\|^2}{\tau^k} \geq \sigma_J \tau^k \frac{\|h^k - \widehat{h}^k(\bar{\tau})\|^2}{\bar{\tau}^2} \geq \frac{\sigma_J \underline{\tau}}{\bar{\tau}^2}\|h^k - \widehat{h}^k(\bar{\tau})\|^2,$$

for all sufficiently large k. Moreover, since the sequence $\{\widehat{J}(h^k) : k \in \mathcal{I}\}$ is monotonically decreasing and $\widehat{J}$ is bounded from below, the conclusion follows.   □

Now we are in a position to present the main result of our convergence analysis.

Theorem 5.9. *Let the sequence $\{(u^k, h^k)\}$ be generated by Algorithm 5.5. In addition, assume that the auxiliary variables $\{w^k\}$, recall (28) and (38) for the respective cases $k \in \mathcal{I}$ and $k \notin \mathcal{I}$ and also see equations (52) and (54) below, are uniformly bounded. Then there exists an accumulation point $\{(u^*, h^*)\}$ which is feasible and C-stationary for (6), i.e. $\{(u^*, h^*)\}$ satisfies (8) and (19) for some $p^* \in (\mathbb{R}^{|\Omega_u|})^2$, $w^* \in (\mathbb{R}^{|\Omega_u|})^2$, $v^* \in \mathbb{R}^{|\Omega_u|}$.*

Proof. The proof is divided into two cases.

Case I. Let us consider the case where $|\mathcal{I}|$ is infinite. In view of Lemma 5.8, let $\{(u^k, h^k, p^k)\}$ be a subsequence (the index k is kept throughout this proof for brevity) such that $k \in \mathcal{I}$ for all k and

$$(51) \qquad \lim_{k \to \infty} \left\| h^k - P_{Q_h}[h^k - \bar{\tau} D_h \widehat{J}(h^k)^\top] \right\| = 0.$$

Let (u^*, h^*, p^*) be an accumulation point of $\{(u^k, h^k, p^k)\}$. Note that (u^*, h^*, p^*) is feasible, i.e. satisfies the state equation (8), owing to the continuity of F and the closedness of G. If strict complementarity holds at (u^*, h^*, p^*), then $\widehat{J}$ is continuously differentiable at h^*, and therefore we have $h^* = P_{Q_h}[h^* - \bar{\tau} D_h \widehat{J}(h^*)^\top]$, or equivalently (u^*, h^*, p^*) is (C-)stationary.

Now assume that (u^*, h^*, p^*) lacks strict complementarity. For each k, let $g^k := D_h \widehat{J}(h^k)^\top$. Then from (27) we have

$$(52) \qquad \begin{cases} g^k = D_h J(u^k, h^k)^\top + D_h F(u^k, h^k)^\top v^k, \\ D_u F(u^k, h^k)^\top v^k + \alpha \nabla^\top w^k + D_u J(u^k, h^k)^\top = 0, \\ w^k = \frac{1}{\alpha}(-I + p^k (p^k)^\top) \eta^k, \\ \alpha \nabla v^k + |\nabla u^k| \eta^k = 0, \end{cases}$$

with $v^k \to v^*$, $g^k \to g^*$, $w^k \to w^*$ as $k \to \infty$, possibly along yet another subsequence.

We claim that $(u^*, h^*, p^*, w^*, v^*)$ satisfies the C-stationarity (20). From (51) and (52), one readily verifies the first and the second conditions in (20). In view of the satisfaction of strict complementarity at each (u^k, h^k, p^k), the proof of the third condition that $(\alpha \nabla^\top w^*, -v^*) \in N_{\mathrm{gph}\, G}^{(\mathrm{C})}(u^*, \alpha \nabla^\top p^*)$ separates into two cases for each $j \in \Omega_u$.

(I-1) There exists a subsequence $\{(u^k, h^k, p^k)\}$ such that $(\nabla u^k)_j \neq 0$ and $|p_j^k| = 1$ for all k. Then it follows from (52) that

$$|(\nabla u^k)_j| w_j^k = (\nabla v^k)_j - \langle (\nabla v^k)_j, p_j^k \rangle p_j^k.$$

Analogous to (39), this eventually yields $\langle w_j^*, (\nabla v^*)_j \rangle \geq 0$ and $(\nabla v^*)_j - \langle (\nabla v^*)_j, p_j^* \rangle p_j^* = 0$.

(I-2) There exists a subsequence $\{(u^k, h^k, p^k)\}$ such that $(\nabla u^k)_j = 0$ and $|p_j^k| < 1$ for all k. Then it follows from (52) that $(\nabla v^*)_j = 0$.

In both cases above, $(\alpha \nabla^\top w^*, -v^*) \in N_{\mathrm{gph}\, G}^{(\mathrm{C})}(u^*, \alpha \nabla^\top p^*)$ holds true.

Case II. Now we turn to the case where $|\mathcal{I}|$ is finite. We claim that $\lim_{k \to \infty} \gamma^k = 0$ in this scenario. Assume for the sake of contradiction that for all sufficiently large k we have $\gamma^k = \bar{\gamma}$ for some $\bar{\gamma} > 0$ and $\|\check{h}^k(\bar{\tau}) - h^k\| > \sigma_h \bar{\gamma}$. Then Algorithm 5.5, for all sufficiently large k, reduces to a projected gradient method on the constrained minimization (35) with a continuously differentiable objective. This leads to a contradiction as $\lim_{k \to \infty} \|\check{h}^k(\bar{\tau}) - h^k\| = 0$ due to Proposition 2 in [22]. Thus, we must have $\lim_{k \to \infty} \gamma^k = 0$.

As a consequence, steps 17–23 in Algorithm 5.5 yields the existence of a subsequence $\{(u^k, h^k)\}$ such that $k \notin \mathcal{I}$ for all k and

$$(53) \qquad \|\check{h}^k(\bar{\tau}) - h^k\| = \left\| h^k - P_{Q_h}[h^k - \bar{\tau} D_h \check{J}_{\gamma^k}(h^k)^\top] \right\| \leq \sigma_h \gamma^k \to 0,$$

as $k \to \infty$. Let $g_\gamma^k := D_h \breve{J}_{\gamma^k}(h^k)^\top$, and we have

(54)
$$\begin{cases} F(u^k, p^k) + \alpha \nabla^\top p_\gamma^k = 0, \\ p_\gamma^k := \varphi'_{\gamma^k}(\nabla u^k), \\ g_\gamma^k = D_h J(u^k, h^k)^\top + D_h F(u^k, h^k)^\top v^k, \\ D_u F(u^k, h^k)^\top v^k + \alpha \nabla^\top w^k = -D_u J(u^k, h^k)^\top, \\ w^k = \varphi''_{\gamma^k}(\nabla u^k) \nabla v^k, \end{cases}$$

for all k such that $h^k \to h^*$, $u^k \to u^*$, $p_\gamma^k \to p^*$, $v^k \to v^*$, $w^k \to w^*$, $g_\gamma^k \to g_\gamma^*$ as $k \to \infty$, possibly along another subsequence. Then from (53) and (54), the first and the second conditions in the C-stationarity condition (20) immediately follow. The satisfaction of the third condition in (20) can be verified using an argument analogous to that in the proof of cases (1)–(3) in Theorem 5.4. Thus, we conclude that (u^*, h^*) is C-stationary. $\square$

6. **Numerical experiments.** In this section, we report our numerical experiments on the bilevel optimization framework for blind deconvolution problems. In order to achieve practical efficiency, in section 6.1.2 we will utilize a simplified version of Algorithm 5.5. In particular, the smoothed lower-level problem can be efficiently handled by a semismooth Newton solver, which is described in section 6.1.1. Numerical results on PSF calibration and multiframe blind deconvolution are given in sections 6.2 and 6.3, respectively.

6.1. **Implementation issues.** Here our concern is to implement a practically efficient version of the hybrid projected gradient method (i.e. Algorithm 5.5) developed in section 5.3. At each iteration of that algorithm, step 14 requires the numerical solution of the set-valued equation (8) for obtaining a feasible point. In this vein, first-order methods are typically used, see, e.g., [11] and its variants, but they only converge sublinearly. We note that the semismooth Newton method without any regularization is not directly applicable for solving (8) due to non-uniqueness in the (dual) variable p. As a remedy, a null-space regularization on the predual problem is introduced in [25]. A more computationally amenable Tikhonov regularization (on the dual problem), which is equivalent to Huber-type smoothing on the primal objective, is proposed in [26]. Following [26], the Euler-Lagrange equation (33) in the smoothing step (i.e. steps 16–26) of Algorithm 5.5 can be solved by a superlinearly convergent semismooth Newton method. To take advantage of this fact, we will simplify Algorithm 5.5 by implementing the smoothing step only in Algorithm 6.2. In the meantime, we first describe a semismooth Newton solver for the smoothed lower-level problem.

6.1.1. *Semismooth Newton solver for the smoothed lower-level problem.* We only present essentials of the semismooth Newton method as a subroutine in solving the bilevel problem and refer the interested reader to [26, 28, 29] for further details. For the smoothed lower-level problem in (32), we fix $\gamma > 0$ and $h \in Q_h$. With the introduction a dual variable $p^\gamma \in \left(\mathbb{R}^{|\Omega_u|}\right)^2$, the Euler-Lagrange equation (33) associated with the smoothing parameter γ can be reformulated as follows:

$$\begin{cases} (-\mu\Delta + K(h)^\top K(h))u^\gamma + \alpha\nabla^\top p^\gamma = K(h)^\top z, \\ \max(|\nabla u^\gamma|, \gamma)p^\gamma = \left(\dfrac{3}{2} - \dfrac{|\nabla u^\gamma|^2}{2\max(|\nabla u^\gamma|, \gamma)^2}\right)\nabla u^\gamma. \end{cases}$$

To ease our presentation, we temporarily omit the superscript γ in u^γ and p^γ, and denote the iterates in the lower-level solver (i.e. inner loop) by (u^l, p^l). A generalized Newton step on the above Euler-Lagrange equation refers to the solution of the following linear system:

$$
\begin{bmatrix} -\mu\Delta + K(h)^\top K(h) & \alpha\nabla^\top \\ -C^l\nabla & \operatorname{diag}(m^l e) \end{bmatrix} \begin{bmatrix} \delta u^l \\ \delta p^l \end{bmatrix}
$$
$$
= \begin{bmatrix} -(-\mu\Delta + K(h)^\top K(h))u^l - \alpha\nabla^\top p^l + K(h)^\top z \\ -m^l p^l + \left(\dfrac{3}{2} - \dfrac{|\nabla u^l|^2}{2(m^l)^2}\right)\nabla u^l \end{bmatrix},
$$

where

$$
m^l := \max(|\nabla u^l|, \gamma),
$$
$$
(\chi^l)_j := \begin{cases} 1 & \text{if } |(\nabla u^l)_j| \geq \gamma \\ 0 & \text{if } |(\nabla u^l)_j| < \gamma \end{cases} \quad \forall j \in \Omega_u,
$$
$$
C^l := \chi^l\left(I - (m^l)^{-1}p^l(\nabla u^l)^\top\right) + (1 - \chi^l)\left(\dfrac{3}{2}I - \operatorname{diag}\left(\dfrac{|\nabla u^l|^2 e}{2\gamma^2}\right) - \dfrac{(\nabla u^l)(\nabla u^l)^\top}{\gamma^2}\right).
$$

After eliminating δp^l in the above Newton system, we arrive at

$$
\left(-\mu\Delta + K(h)^\top K(h) + \alpha\nabla^\top (m^l)^{-1}C^l\nabla\right)\delta u^l = -r(u^l; h, \gamma),
$$

recall (33) for the definition of the residual term $r(\cdot)$. In order to guarantee that δu^l be a descent direction for the lower-level minimization problem, we further introduce a modification on C^l, i.e. we replace C^l by

$$
\widehat{C}^l := \chi^l\left(I - \dfrac{1}{2}(m^l)^{-1}\left(\widehat{p}^l(\nabla u^l)^\top + (\nabla u^l)(\widehat{p}^l)^\top\right)\right)
$$
$$
+ (1 - \chi^l)\left(\dfrac{3}{2}I - \operatorname{diag}\left(\dfrac{|\nabla u^l|^2 e}{2\gamma^2}\right) - \dfrac{(\nabla u^l)(\nabla u^l)^\top}{\gamma^2}\right),
$$

where $\widehat{p}^l$ is the projection of p^l onto Q_p, i.e. $\widehat{p}^l := \dfrac{p^l}{\max(|p^l|, 1)}$. Thus, the final modified Newton system appears as

$$
(55) \qquad \left(-\mu\Delta + K(h)^\top K(h) + \alpha\nabla^\top (m^l)^{-1}\widehat{C}^l\nabla\right)\delta u^l = -r(u^l; h, \gamma).
$$

Once δu^l is obtained, δp^l can be computed by

$$
(56) \qquad \delta p^l := -p^l + (m^l)^{-1}\left(\dfrac{3}{2} - \dfrac{|\nabla u^l|^2}{2(m^l)^2}\right)\nabla u^l + (m^l)^{-1}\widehat{C}^l\nabla\delta u^l.
$$

The overall semismooth Newton solver for the smoothed lower-level problem is summarized in Algorithm 6.1 below. The superlinear convergence of this solver can be justified following the approach in [26, 28].

Algorithm 6.1 (Semismooth Newton solver).
Require: (ordered) inputs $\alpha > 0$, $0 < \mu \ll \alpha$, $h \in Q_h$, $\gamma > 0$, $u^1 \in \mathbb{R}^{|\Omega_u|}$, $\operatorname{tol}_r > 0$.
    Return: $u^* \in \mathbb{R}^{|\Omega_u|}$.
  1: Initialize $p^1 := \dfrac{\nabla u^1}{\max(|\nabla u^1|, \gamma)}$, $l := 1$.
  2: **loop**
  3:     Generate the Newton system in (55).
  4:     **if** $\dfrac{\|r(u^l; h, \gamma)\|}{\max(\|r(u^1; h, \gamma)\|, 1)} \leq \operatorname{tol}_r$ **then**

5:      return $u^* := u^l$ and terminate the algorithm.
6:   **end if**
7:   Solve (55) for δu^l, and compute δp^l using formula (56).
8:   Determine the step size $a^l > 0$ via backtracking Armijo line search along δu^l.

9:   Generate the next iterates: $u^{l+1} := u^l + a^l \delta u^l$ and $p^{l+1} := p^l + a^l \delta p^l$.
10: Set $l := l + 1$.
11: **end loop**

6.1.2. *Simplified projected gradient method.* Based on Algorithm 6.1, we present the simplified projected gradient method for the bilevel problem (6) in the following. We remark that while the proximity measure κ^k in step 3 is chosen in our algorithm as a signal for reducing γ^k, other choices may be considered as well.

Algorithm 6.2 (Simplified projected gradient method).
Require: inputs $\alpha > 0$, $0 < \mu \ll \alpha$, $\mathrm{tol}_r > 0$, $0 < \sigma_J < 1$, $\sigma_h > 0$, $\bar{\tau} > 0$, $\mathrm{tol}_\gamma > 0$,
      $0 < \rho_\gamma < 1$, $0 < \rho_\tau < 1$.
1: Initialize $h^1 \in Q_h$, $\gamma^1 > 0$, $u^0 \in \mathbb{R}^{|\Omega_u|}$, $k := 1$.
2: **loop**
3:   Apply Algorithm 6.1 with ordered inputs α, μ, h^k, γ^k, u^{k-1}, tol_r, which
      returns u^k as the solution of (33).
4:   Solve the adjoint equation

$$\left(D_u F(u^k, h^k)^\top + \alpha \nabla^\top \varphi''_{\gamma^k}(\nabla u^k)\nabla \right) v^k = -D_u J(u^k, h^k)^\top$$

      for v^k. Then compute the gradient $D_h \breve{J}_{\gamma^k}(h^k)^\top := D_h J(u^k, h^k)^\top + D_h F(u^k,$
      $h^k)^\top v^k$ and evaluate the proximity measure

$$\kappa^k := \left\| P_{Q_h}[h^k - \bar{\tau} D_h \breve{J}_{\gamma^k}(h^k)^\top] - h^k \right\|.$$

5:   **if** $\kappa^k \leq \sigma_h \gamma^k$ **then**
6:      **if** $\gamma^k = \mathrm{tol}_\gamma$ **then**
7:         return (u^k, h^k) as a C-stationary point of (6) and terminate the algo-
            rithm.
8:      **else**
9:         Set $\gamma^{k+1} := \max(\rho_\gamma \gamma^k, \mathrm{tol}_\gamma)$. Go to step 13.
10:     **end if**
11: **end if**
12: Set $h^{k+1} := P_{Q_h}[h^k - \tau^k D_h \breve{J}_{\gamma^k}(h^k)^\top]$, where τ^k the largest element in $\{\bar{\tau}(\rho_\tau)^l :$
      $l = 0, 1, 2, ...\}$ which fulfills the following Armijo-type condition:

$$\breve{J}_{\gamma^k}\left(P_{Q_h}[h^k - \tau^k D_h \breve{J}_{\gamma^k}(h^k)^\top] \right)$$
$$\leq \breve{J}_{\gamma^k}(h^k) + \sigma_J D_h \breve{J}_{\gamma^k}(h^k)(P_{Q_h}[h^k - \tau^k D_h \breve{J}_{\gamma^k}(h^k)^\top] - h^k).$$

13: Set $k := k + 1$.
14: **end loop**

We further specify the parameter choices for Algorithm 6.2 in our numerical experiments. The image intensity is scaled to $[0, 1]$ in all examples. For an image

of $n_x \times n_y$ pixels, we set the mesh size $\omega := \sqrt{1/(n_x n_y)}$ and discretize the spatial gradient by forward differences, i.e. for each $j = (j_x, j_y) \in \Omega_u$,

$$(\nabla u)_{(j_x, j_y)} := \left(\frac{u_{(j_x+1, j_y)} - u_{(j_x, j_y)}}{\omega}, \frac{u_{(j_x, j_y+1)} - u_{(j_x, j_y)}}{\omega} \right)$$

with homogenous Dirichlet boundary condition. The following parameters are chosen throughout the experiments: $\alpha = 10^{-5}$, $\mu = 10^{-4}\alpha$, $\sigma_J = \sigma_h = 0.01$, $\rho_\gamma = \rho_\tau = 1/2$, $u^0 = z$, $\gamma^1 = 0.05/\omega$, $\text{tol}_\gamma = 0.001/\omega$, $\text{tol}_r = 10^{-7}$. The conjugate gradient method is utilized for solving the linear systems in step 3 of Algorithm 6.1 with residual tolerance 0.01 and in step 3 of Algorithm 6.2 with residual tolerance 10^{-9}, respectively. All experiments are performed under Matlab R2011b.

6.2. **Calibration of point spread functions.** We first test our method on a point spread function (PSF) calibration problem. Let h be a point spread function on a 2D index domain Ω_h, and $Q_h = \{h \in \mathbb{R}^{|\Omega_h|} : \sum_{j \in \Omega_h} h_j = 1, \ h_j \geq 0 \ \forall j \in \Omega_h\}$. The blurring operator K is defined through a 2D convolution, i.e. $K(h)u = h * u$, with zero boundary condition. Given the true PSF $h_{(\text{true})} \in Q_h$ and the source image $u_{(\text{true})} \in \mathbb{R}^{|\Omega_u|}$, the observed image z is generated as $h_{(\text{true})} * u_{(\text{true})} + \text{noise}$, where the noise is white Gaussian and of zero mean and standard deviation 0.02. In addition to the observation, we are supplied with a reference image $u_{(\text{ref})}$, which is generated as the (non-blurred) source image corrupted by white Gaussian noise of zero mean and standard deviation 0.1. Our aim is to calibrate the underlying PSF using a blurred observation image and a noisy reference image.

In this problem, we utilize a tracking-type objective

$$J(u, h) = \frac{1}{2}\|u - u_{(\text{ref})}\|^2 + \frac{\beta}{2}\|\nabla h\|^2$$

in the upper level, where a Tikhonov regularization on h is also included to stabilize the solution and the regularization parameter $\beta = 0.05$ is chosen. We remark that alternative regularizations on h, e.g. total-variation regularization [13], might be favorable for certain classes of PSFs. The relevant partial derivatives of J and F required for the implementation of Algorithm 6.2 are listed below

$$D_u J(u, h)^\top = u - u_{(\text{ref})},$$
$$D_h J(u, h)^\top = -\beta \Delta h,$$
$$(57) \qquad D_u F(u, h)^\top = (-\mu \Delta + K(h)^\top K(h)),$$
$$(58) \qquad \langle D_h F(u, h)^\top v, \delta h \rangle = \langle v, D_h F(u, h) \delta h \rangle$$
$$\qquad\qquad = \langle v, \delta h(-\cdot) * (h * u - z) \rangle + \langle v, h(-\cdot) * (\delta h * u) \rangle.$$

Here $h(-\cdot)$ is a PSF in Q_h defined by $(h(-\cdot))_j = h_{-j}$ for all $j \in \Omega_h$, and similar for $\delta h(-\cdot)$. The size of Ω_h is always chosen to be slightly larger than the support size of the true PSF. Note that for $D_h F(u, h)^\top$ only the matrix-vector product $D_h F(u, h)^\top v$ is needed in the numerical computation, which is given by (58) in a dual form. The projection $P_{Q_h}[\cdot]$ in Algorithm 6.2 requires solving a quadratic program and can be efficiently computed by standard routines such as `quadprog` in Matlab. Concerning the initializations, we set the initial line search step size $\bar{\tau} = 2 \times 10^{-5}$ and the initial PSF h^1 to be the discrete Dirac delta function.

Our experiments are performed on three different pairs of images and PSFs, namely Gaussian blur on the "Satellite" image, motion blur on the "Cameraman" image, and out-of-focus blur on the "Grain" image. In Figure 1, the ground-truth

images are displayed in (a)–(c), the underlying PSFs in (d)–(f), and the corresponding blurred observations in (g)–(i). The results of the bilevel-optimization calibration are shown in the last two rows: (j)–(l) for the estimated PSFs and (m)–(o) for the deblurred images from the lower-level problem. It is observed that the calibrations are reasonably good in all three cases in the sense that the calibrated PSFs resemble their true counterparts and yield the deblurred images of high visual quality.
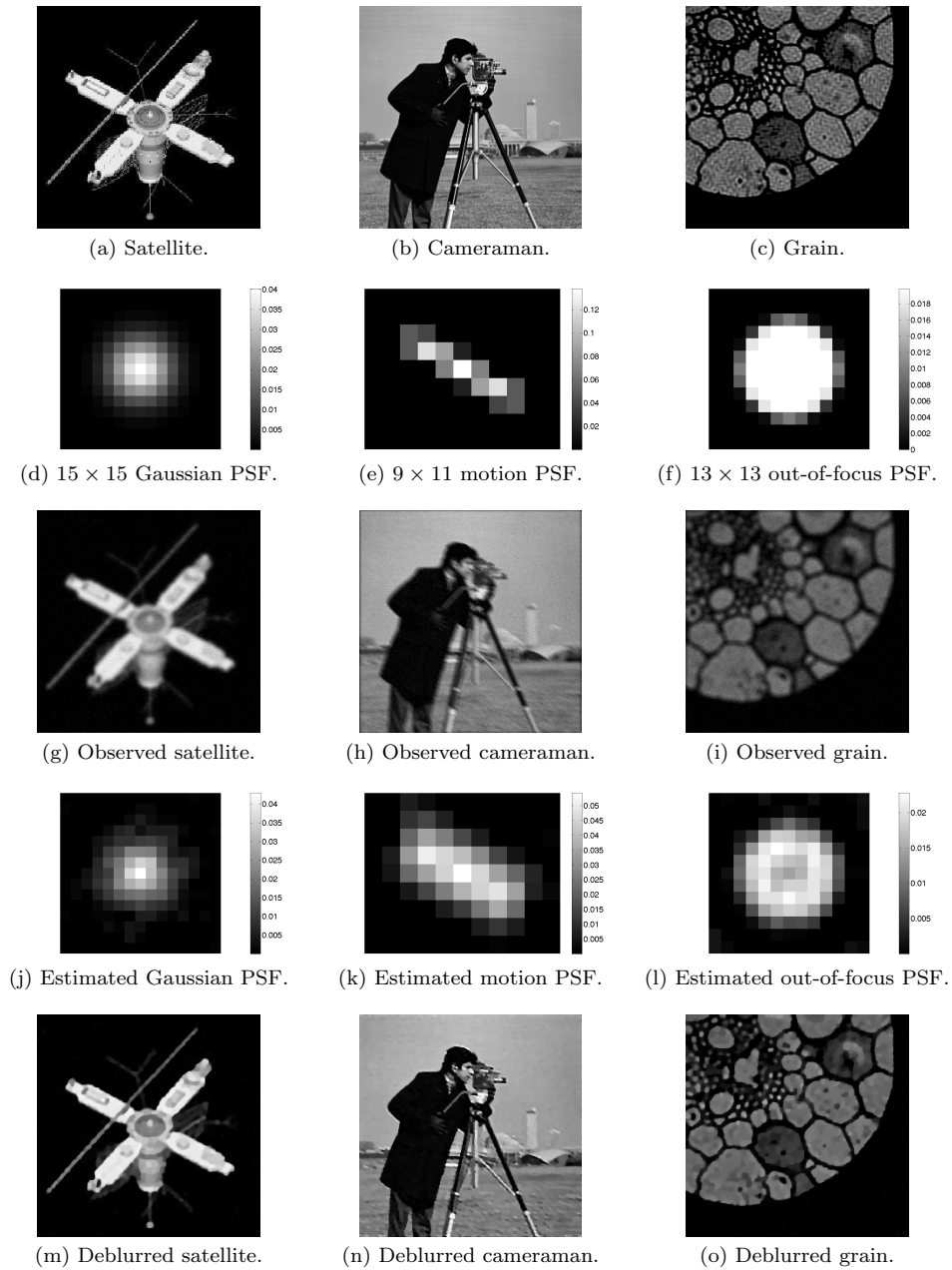

(a) Satellite. (b) Cameraman. (c) Grain.

(d) 15×15 Gaussian PSF. (e) 9×11 motion PSF. (f) 13×13 out-of-focus PSF.

(g) Observed satellite. (h) Observed cameraman. (i) Observed grain.

(j) Estimated Gaussian PSF. (k) Estimated motion PSF. (l) Estimated out-of-focus PSF.

(m) Deblurred satellite. (n) Deblurred cameraman. (o) Deblurred grain.

FIGURE 1. Calibration of point spread functions.

In Figure 2, we also illustrate the typical numerical behavior of Algorithm 6.2 in the "satellite" example. Subplot (a) records the history of the smoothing parameter γ^k. The objective values $J(u^k, h^k)$ are shown in (b), which exhibit regular decrease along iterations. The proximity measure κ^k in step 4 of Algorithm 6.2, shown in subplot (c), also behaves well.

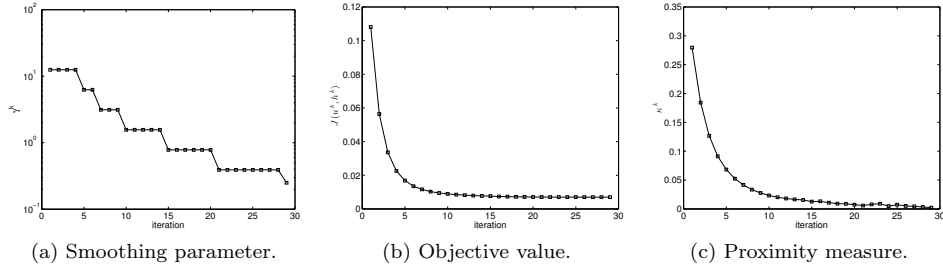(a) Smoothing parameter.　　(b) Objective value.　　(c) Proximity measure.

FIGURE 2. Numerical behavior.

6.2.1. *Comparison with a single-level optimization approach.* Here we compare our bilevel approach with a single-level alternating minimization method, in the spirit of [53, 13, 23], for calibrating PSFs. More precisely, one considers the following model:

$$\text{minimize} \quad J_\lambda(u, h) := \frac{\mu}{2}\|\nabla u\|^2 + \frac{1}{2}\|h * u - z\|^2 + \alpha\|\nabla u\|_{1,\gamma}$$
$$+ \lambda\left(\frac{1}{2}\|u - u_{(\text{ref})}\|^2 + \frac{\beta}{2}\|\nabla h\|^2\right)$$
$$\text{over} \quad u \in \mathbb{R}^{|\Omega_u|}, \ h \in Q_h.$$

The objective J_λ combines the upper-level and lower-level objectives in the bilevel model with a balancing weight $\lambda > 0$. Fixing λ, to obtain a numerical solution for this model, one may utilize an alternating minimization scheme [13] formulated in the following.

Algorithm 6.3 (Single-level alternating minimization).
1: Initialize $k := 0$ and h^0 as the discrete Dirac delta function.
2: **repeat**
3:　　Compute $u^{k+1} := \arg\min_{u \in \mathbb{R}^{|\Omega_u|}} J_\lambda(u, h^k)$.
4:　　Compute $h^{k+1} := \arg\min_{h \in Q_h} J_\lambda(u^{k+1}, h)$.
5:　　Set $k := k + 1$.
6: **until** some stopping criterion is satisfied.

In Algorithm 6.3, step 3 calls for the solution of the following optimality system:

$$-\mu\Delta u^{k+1} + h^k(-\cdot) * (h^k * u^{k+1} - z) + \alpha\nabla^\top(\varphi'_\gamma(\nabla u^{k+1})) + \lambda(u^{k+1} - u_{(\text{ref})}) = 0,$$

which can be carried out by a simple adaption of the semismooth Newton method in Algorithm 6.1. Meanwhile, step 4 corresponds to a standard quadratic programm. Thus, the computational cost of each iteration in the single-level approach roughly equals that in the bilevel approach in Algorithm 6.2. We terminate Algorithm 6.3 once $(J_\lambda(u^k, h^k) - J_\lambda(u^{k+1}, h^{k+1}))/J_\lambda(u^k, h^k) < 10^{-6}$.

Figure 3 demonstrates the comparison between our bilevel approach in Algorithm 6.2 and the single-level approach in Algorithm 6.3 on the "Grain" example under

exactly the same experimental setting as before. One difficulty for the single-level approach is that the proper choice of the additional weight parameter λ remains unclear. In our experiments, we have run the single-level approach with a series of different λ's. The resulting relative mean squared errors (RMSE) on the PSF $h(\lambda)$, measured by $\|h(\lambda) - h_{(\text{true})}\| / \|h_{(\text{true})}\|$, for each λ are plotted in subplot (d). The PSF via the single-level model reaches the smallest RMSE (=0.1481) when $\lambda = 0.05$, which is shown in subplot (c). It is observed that the bilevel model yields a PSF, see subplot (b), which is both visually and numerically (RMSE=0.1560) close to the PSF via the single-level model with the optimally chosen λ. Otherwise, the bilevel model is always superior, with respect to RMSE on PSF, over single-level models with non-optimal λ's. Thus, our bilevel approach is favorable for its automation in the sense that it avoids selection of the additional parameter λ which is often done by trail and error.
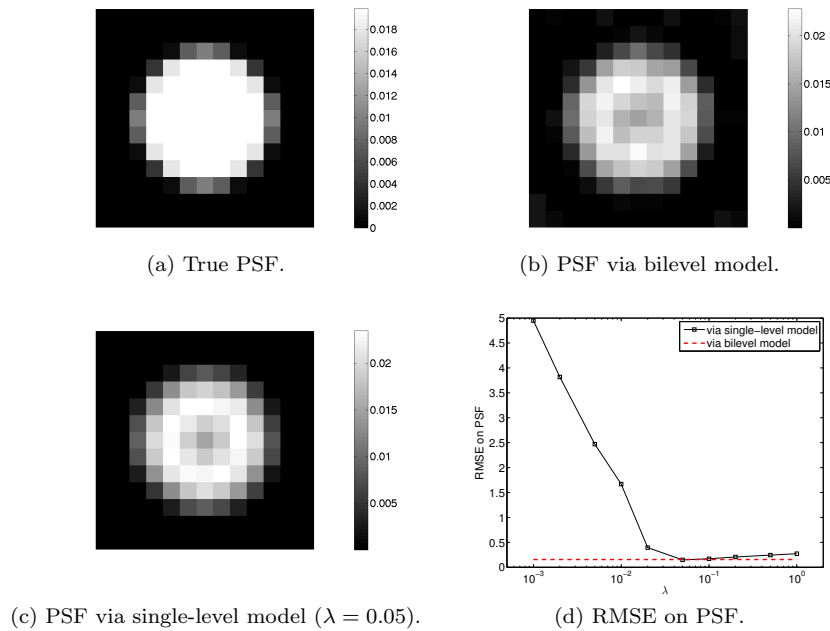

(a) True PSF.

(b) PSF via bilevel model.

(c) PSF via single-level model ($\lambda = 0.05$).

(d) RMSE on PSF.

FIGURE 3. Comparison with single-level alternating minimization.

6.3. **Multiframe blind deconvolution.** Now we apply our algorithmic framework to *multiframe blind deconvolution* [6]. In this problem, the observation $\vec{z}$ consists of f frames, i.e. $\vec{z} = (\vec{z}^1, ..., \vec{z}^f)$, where each frame is generated from the convolution between the source image $u_{(\text{true})}$ and a frame-varying PSF $\vec{h}^i$ over Ω_h plus some additive Gaussian noise $\vec{\eta}^i$, i.e.

$$\vec{z}^i = \vec{h}^i * u_{(\text{true})} + \vec{\eta}^i, \quad \forall i \in \{1, 2, ..., f\}.$$

Furthermore, each PSF $\vec{h}^i$ follows a (normalized) multivariate Gaussian distribution, i.e. $\vec{h}^i = h(\vec{\sigma}_x^i, \vec{\sigma}_y^i, \vec{\theta}^i)$ with unknown frame-dependent parameters $\vec{\sigma}_x^i, \vec{\sigma}_y^i \in Q_\sigma$, $\vec{\theta}^i \in Q_\theta$. The parameterization of the Gaussian PSF $h : Q_\sigma \times Q_\sigma \times Q_\theta \to Q_h$ is defined

by

$$h(\sigma_x, \sigma_y, \theta) := \frac{\widetilde{h}(\sigma_x, \sigma_y, \theta)}{\sum_{(j_x, j_y) \in \Omega_h} \left(\widetilde{h}(\sigma_x, \sigma_y, \theta)\right)_{(j_x, j_y)}},$$

where for all $(j_x, j_y) \in \Omega_h$

$$\left(\widetilde{h}(\sigma_x, \sigma_y, \theta)\right)_{(j_x, j_y)} := \frac{1}{2\pi\sigma_x\sigma_y} \exp\left(-\frac{(j_x\cos\theta - j_y\sin\theta)^2}{2(\sigma_x)^2} - \frac{(j_x\sin\theta + j_y\cos\theta)^2}{2(\sigma_y)^2}\right).$$

Our task is to simultaneously recover the image $u_{(\text{true})}$ and the PSF parameters $\vec{\sigma}_x, \vec{\sigma}_y \in (Q_\sigma)^f$ and $\vec{\theta} \in (Q_\theta)^f$.

For such a multiframe blind deconvolution problem, we formulate the bilevel optimization model as follows:

$$\begin{aligned}
\min \quad & J(\vec{u}) = \frac{1}{2}\sum_{k=1}^{f}\left\|\vec{u}^k - \frac{1}{f}\sum_{l=1}^{f}\vec{u}^l\right\|^2 \\
\text{s.t.} \quad & \vec{u}^i = \arg\min_{u \in \mathbb{R}^{|\Omega_u|}} \frac{1}{2}\left\|h(\vec{\sigma}_x^i, \vec{\sigma}_y^i, \vec{\theta}^i) * u - \vec{z}^i\right\|^2 + \alpha\|\nabla u\|_1, \quad \forall i \in \{1, 2, ...f\}, \\
& \vec{\sigma}_x, \vec{\sigma}_y \in (Q_\sigma)^f, \ \vec{\theta} \in (Q_\theta)^f.
\end{aligned}$$

The upper-level objective represents a (rescaled) sample variance of $\{\vec{u}^1, ..., \vec{u}^f\}$. Upon Huber-type smoothing on each lower-level problem respectively, the derivative of the reduced objective $\widehat{J}(\vec{\sigma}_x, \vec{\sigma}_y, \vec{\theta}) := J(\vec{u}^1(\vec{\sigma}_x^1, \vec{\sigma}_y^1, \vec{\theta}^1), ..., \vec{u}^f(\vec{\sigma}_x^f, \vec{\sigma}_y^f, \vec{\theta}^f))$ can be calculated for all $i \in \{1, ..., f\}$ as

$$D_{(\vec{\sigma}_x^i, \vec{\sigma}_y^i, \vec{\theta}^i)}\widehat{J}(\vec{\sigma}_x, \vec{\sigma}_y, \vec{\theta})^\top = D_{(\sigma_x, \sigma_y, \theta)}h(\vec{\sigma}_x^i, \vec{\sigma}_y^i, \vec{\theta}^i)^\top D_h F(\vec{u}^i, \vec{h}^i)^\top \vec{v}^i,$$

where each $\vec{v}^i \in \mathbb{R}^{|\Omega_u|}$ satisfies the adjoint equation

$$\left(D_u F(\vec{u}^i, \vec{h}^i)^\top + \alpha\nabla^\top \varphi_\gamma''(\nabla\vec{u}^i)\nabla\right)\vec{v}^i = -D_{\vec{u}^i}J(\vec{u})^\top = -\left(\vec{u}^i - \frac{1}{f}\sum_{l=1}^{f}\vec{u}^l\right).$$

In addition, the formulae for $D_u F(\cdot)^\top$ and $D_h F(\cdot)^\top$ are identical to (57) and (58), and the partial derivatives of h are respectively given by

$$\left(D_{\sigma_x}\widetilde{h}(\sigma_x, \sigma_y, \theta)^\top\right)_{(j_x, j_y)} = \left(\widetilde{h}(\sigma_x, \sigma_y, \theta)\right)_{(j_x, j_y)}\left(\frac{(j_x\cos\theta - j_y\sin\theta)^2}{(\sigma_x)^3} - \frac{1}{\sigma_x}\right),$$

$$D_{\sigma_x}h(\sigma_x, \sigma_y, \theta)^\top = \frac{1}{\sum_{(j_x, j_y) \in \Omega_h}\left(\widetilde{h}(\sigma_x, \sigma_y, \theta)\right)_{(j_x, j_y)}} \cdot$$

$$\left(D_{\sigma_x}\widetilde{h}(\sigma_x, \sigma_y, \theta)^\top - h(\sigma_x, \sigma_y, \theta)\sum_{(j_x, j_y) \in \Omega_h}\left(D_{\sigma_x}\widetilde{h}(\sigma_x, \sigma_y, \theta)^\top\right)_{(j_x, j_y)}\right),$$

$$\left(D_{\sigma_y}\widetilde{h}(\sigma_x, \sigma_y, \theta)^\top\right)_{(j_x, j_y)} = \left(\widetilde{h}(\sigma_x, \sigma_y, \theta)\right)_{(j_x, j_y)}\left(\frac{(j_x\sin\theta + j_y\cos\theta)^2}{(\sigma_y)^3} - \frac{1}{\sigma_y}\right),$$

$$D_{\sigma_y}h(\sigma_x, \sigma_y, \theta)^\top = \frac{1}{\sum_{(j_x, j_y) \in \Omega_h}\left(\widetilde{h}(\sigma_x, \sigma_y, \theta)\right)_{(j_x, j_y)}} \cdot$$

$$\left(D_{\sigma_y}\widetilde{h}(\sigma_x, \sigma_y, \theta)^\top - h(\sigma_x, \sigma_y, \theta)\sum_{(j_x, j_y) \in \Omega_h}\left(D_{\sigma_y}\widetilde{h}(\sigma_x, \sigma_y, \theta)^\top\right)_{(j_x, j_y)}\right),$$

$$\left(D_\theta \widetilde{h}(\sigma_x, \sigma_y, \theta)^\top \right)_{(j_x, j_y)} = \left(\widetilde{h}(\sigma_x, \sigma_y, \theta) \right)_{(j_x, j_y)} \left(\frac{1}{(\sigma_x)^2} - \frac{1}{(\sigma_y)^2} \right) \cdot$$
$$(j_x \cos\theta - j_y \sin\theta)(j_x \sin\theta + j_y \cos\theta),$$

$$D_\theta h(\sigma_x, \sigma_y, \theta)^\top = \frac{1}{\sum_{(j_x, j_y) \in \Omega_h} \left(\widetilde{h}(\sigma_x, \sigma_y, \theta) \right)_{(j_x, j_y)}} \cdot$$

$$\left(D_\theta \widetilde{h}(\sigma_x, \sigma_y, \theta)^\top - h(\sigma_x, \sigma_y, \theta) \sum_{(j_x, j_y) \in \Omega_h} \left(D_\theta \widetilde{h}(\sigma_x, \sigma_y, \theta)^\top \right)_{(j_x, j_y)} \right) \cdot$$

(a) True PSF #1.　(b) True PSF #2.　(c) True PSF #3.　(d) True PSF #4.

(e) Estimated PSF #1.　(f) Estimated PSF #2.　(g) Estimated PSF #3.　(h) Estimated PSF #4.

(i) True PSF #5.　(j) True PSF #6.　(k) True PSF #7.　(l) True PSF #8.

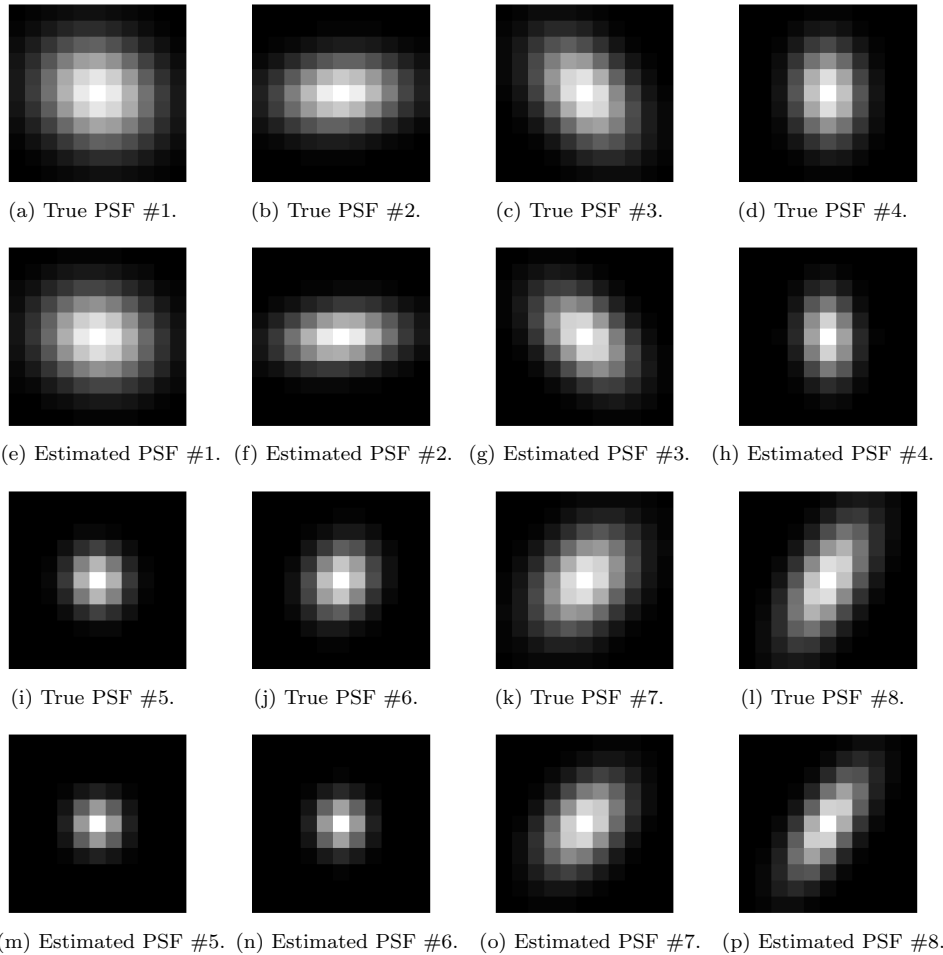(m) Estimated PSF #5.　(n) Estimated PSF #6.　(o) Estimated PSF #7.　(p) Estimated PSF #8.

FIGURE 4. Multiframe blind deconvolution — PSFs.

In our experiments, $Q_\sigma = [1,3]$ and $Q_\theta = [-\pi/2, \pi/2]$ are fixed, and the underlying parameters $(\vec{\sigma}_x^{(\text{true})}, \vec{\sigma}_y^{(\text{true})}, \vec{\theta}^{(\text{true})})$ are (uniform-)randomly drawn from $(Q_\sigma)^f \times (Q_\sigma)^f \times (Q_\theta)^f$. The first and third rows of Figure 4 show the random PSFs in a trial run with 8 frames, i.e. $f = 8$. The corresponding observations are given in the first

(a) Observation #1.   (b) Observation #2.   (c) Observation #3.   (d) Observation #4.

(e) Deblurred frame #1.   (f) Deblurred frame #2.   (g) Deblurred frame #3.   (h) Deblurred frame #4.

(i) Observation #5.   (j) Observation #6.   (k) Observation #7.   (l) Observation #8.

(m) Deblurred frame #5.   (n) Deblurred frame #6.   (o) Deblurred frame #7.   (p) Deblurred frame #8.

FIGURE 5. Multiframe blind deconvolution — images.

and third rows of Figure 5. Concerning the initializations in our implementation, we always choose $\bar{\tau} = 0.005$ and $(\vec{\sigma}_x^i)^1 = (\vec{\sigma}_y^i)^1 = 2$, $(\vec{\theta}^i)^1 = 0$ for all i.

The results of the 8-frame trial run, both PSFs and images, are displayed in Figures 4 and 5 respectively. It is observed from the comparison in Figure 4 that our method well captures the underlying PSFs, especially the widths and the orientations in case of strongly skewed PSFs (see #2, #3, #4, #7, #8). Furthermore, all deblurred frames yield significant improvement in visual quality over the corresponding observations.

We are also interested in the effect of the number of frames on the image restoration quality. For this sake, we track the mean peak signal-to-noise ratio (mPSNR) of all individual frames for $f \in \{4, 6, 8, 10, 12\}$. For each f, the mean and the standard deviation (stdev) of mPSNR after 10 trial runs are reported in Table 1, where the mean is rising and the standard deviation is falling as f becomes larger. Thus, we conclude from our experiments that, as is expected, more observations typically enhance the frame-wise image restoration quality in the bilevel-optimization based multiframe blind deconvolution.

f	4	6	8	10	12
mean	23.6019	23.7170	23.7639	23.7883	24.0026
stdev	0.6020	0.4380	0.3381	0.2889	0.2720

Table 1. Mean peak signal-to-noise ratio.

REFERENCES

[1] M. S. C. Almeida and L. B. Almeida, Blind and semi-blind deblurring of natural images, *IEEE Trans. Image Process.,* **19** (2010), 36–52.

[2] G. Aubert and P. Kornprobst, *Mathematical Problems in Image Processing*, Springer, New York, 2002.

[3] J. Bardsley, S. Jefferies, J. Nagy and R. Plemmons, A computational method for the restoration of images with an unknown, spatially-varying blur, *Opt. Express,* **14** (2006), 1767–1782.

[4] M. Burger and O. Scherzer, Regularization methods for blind deconvolution and blind source separation problems, *Math. Control Signals Systems,* **14** (2001), 358–383.

[5] J.-F. Cai, H. Ji, C. Liu and Z. Shen, Blind motion deblurring using multiple images, *J. Comput. Phys.,* **228** (2009), 5057–5071.

[6] P. Campisi and K. Egiazarian, eds., *Blind image deconvolution: Theory and applications*, CRC press, Boca Raton, FL, 2007.

[7] A. S. Carasso, Direct blind deconvolution, *SIAM J. Appl. Math.,* **61** (2001), 1980–2007.

[8] ———, The APEX method in image sharpening and the use of low exponent Lévy stable laws, *SIAM J. Appl. Math.,* **63** (2002), 593–618.

[9] ———, APEX blind deconvolution of color Hubble space telescope imagery and other astronomical data, *Optical Engineering,* **45** (2006), 107004.

[10] ———, False characteristic functions and other pathologies in variational blind deconvolution: A method of recovery, *SIAM J. Appl. Math.,* **70** (2009), 1097–1119.

[11] A. Chambolle and T. Pock, A first-order primal-dual algorithm for convex problems with applications to imaging, *J. Math. Imaging Vis.,* **40** (2011), 120–145.

[12] T. F. Chan and J. Shen, *Image Processing and Analysis: Variational, PDE, Wavelet, and Stochastic Methods*, SIAM, Philadelphia, 2005.

[13] T. F. Chan and C.-K. Wong, Total variation blind deconvolution, *IEEE Trans. Image Process.,* **7** (1998), 370–375.

[14] R. Chartrand and W. Yin, Iteratively reweighted algorithms for compressive sensing, in *Proceedings of the IEEE International Conference on Acoustics,* Speech and Signal Processing, 2008, 3869–3872.

[15] S. Cho, Y. Matsushita and S. Lee, Removing non-uniform motion blur from images, in *IEEE 11th International Conference on Computer Vision,* 2007, 1–8.

[16] J. C. De los Reyes and C.-B. Schönlieb, Image denoising: Learning the noise model via nonsmooth PDE-constrained optimization, *Inverse Problems and Imaging,* **7** (2013), 1183–1214.

[17] A. L. Dontchev and R. T. Rockafellar, Robinson's implicit function theorem and its extensions, *Math. Program., Ser. B,* **117** (2009), 129–147.

[18] D. A. Fish, A. M. Brinicombe and E. R. Pike, Blind deconvolution by means of the Richardson–Lucy algorithm, *J. Opt. Soc. Am. A,* **12** (1995), 58–65.

[19] R. Fletcher, S. Leyffer, D. Ralph and S. Scholtes, Local convergence of SQP methods for mathematical programs with equilibrium constraints, *SIAM J. Optim.,* **17** (2006), 259–286.

[20] R. W. Freund and N. M. Nachtigal, QMR: A quasi-minimal residual method for non-Hermitian linear systems, *Numer. Math.,* **60** (1991), 315–339.

[21] M. Fukushima, Z.-Q. Luo and J.-S. Pang, A globally convergent sequential quadratic programming algorithm for mathematical programs with linear complementarity constraints, *Comput. Optim. Appl.,* **10** (1998), 5–34.

[22] E. M. Gafni and D. P. Bertsekas, *Convergence of a Gradient Projection Method*, Laboratory for Information and Decision Systems Report LIDS-P-1201, Massachusetts Institute of Technology, 1982.

[23] L. He, A. Marquina and S. J. Osher, Blind deconvolution using TV regularization and Bregman iteration, *International Journal of Imaging Systems and Technology,* **15** (2005), 74–83.

[24] M. Hintermüller and I. Kopacka, Mathematical programs with complementarity constraints in function space: C- and strong stationarity and a path-following algorithm, *SIAM J. Optim.,* **20** (2009), 868–902.

[25] M. Hintermüller and K. Kunisch, Total bounded variation regularization as a bilaterally constrained optimization problem, *SIAM J. Appl. Math.,* **64** (2004), 1311–1333.

[26] M. Hintermüller and G. Stadler, An infeasible primal-dual algorithm for total bounded variation-based inf-convolution-type image restoration, *SIAM J. Sci. Comput.,* **28** (2006), 1–23.

[27] M. Hintermüller and T. Surowiec, A bundle-free implicit programming approach for a class of MPECs in function space, preprint, 2014.

[28] M. Hintermüller and T. Wu, Nonconvex TV^q-models in image restoration: Analysis and a trust-region regularization–based superlinearly convergent solver, *SIAM J. Imaging Sci.,* **6** (2013), 1385–1415.

[29] _____ , A superlinearly convergent R-regularized Newton scheme for variational models with concave sparsity-promoting priors, *Comput. Optim. Appl.,* **57** (2014), 1–25.

[30] K. Ito and K. Kunisch, An active set strategy based on the augmented Lagrangian formulation for image restoration, *ESAIM Math. Model. Num.,* **33** (1999), 1–21.

[31] L. Justen, *Blind Deconvolution: Theory, Regularization and Applications*, Ph.D. thesis, University of Bremen, 2006.

[32] L. Justen and R. Ramlau, A non-iterative regularization approach to blind deconvolution, *Inverse Problems,* **22** (2006), 771–800.

[33] D. Kundur and D. Hatzinakos, Blind image deconvolution, *IEEE Signal Process. Mag.,* **13** (1996), 43–64.

[34] _____ , Blind image deconvolution revisited, *IEEE Signal Process. Mag.,* **13** (1996), 61–63.

[35] K. Kunisch and T. Pock, A bilevel optimization approach for parameter learning in variational models, *SIAM J. Imaging Sci.,* **6** (2013), 938–983.

[36] A. Levin, Blind motion deblurring using image statistics, *Advances in Neural Information Processing Systems,* **19** (2006), 841–848.

[37] A. B. Levy, Solution sensitivity from general principles, *SIAM J. Control Optim.,* **40** (2001), 1–38.

[38] Z.-Q. Luo, J.-S. Pang and D. Ralph, *Mathematical Programs with Equilibrium Constraints*, Cambridge University Press, 1996.

[39] B. S. Mordukhovich, *Variational Analysis and Generalized Differentiation, I: Basic Theory, II: Applications*, Springer, 2006.

[40] J. Nocedal and S. Wright, *Numerical optimization*, 2nd ed., Springer, New York, 2006.

[41] J. Outrata, M. Kocvara and J. Zowe, *Nonsmooth Approach to Optimization Problems with Equilibrium Constraints*, Kluwer Academic Publishers, Dordrecht, The Netherlands, 1998.

[42] J. V. Outrata, A generalized mathematical program with equilibrium constraints, *SIAM J. Control Optim.,* **38** (2000), 1623–1638.

[43] S. M. Robinson, Strongly regular generalized equations, *Math. Oper. Res.,* **5** (1980), 43–62.

[44] _____ , Local structure of feasible sets in nonlinear programming, Part III: Stability and sensitivity, *Math. Programming Stud.,* **30** (1987), 45–66.

[45] R. T. Rockafellar and R. J.-B. Wets, *Variational Analysis*, Springer, New York, 1998.

[46] L. Rudin, S. Osher and E. Fatemi, Nonlinear total variation based noise removal algorithms, *Physica D,* **60** (1992), 259–268.

[47] H. Scheel and S. Scholtes, Mathematical programs with complementarity constraints: Stationarity, optimality, and sensitivity, *Math. Oper. Res.,* **25** (2000), 1–22.

[48] S. Scholtes, Convergence properties of a regularization scheme for mathematical programs with complementarity constraints, *SIAM J. Optim.,* **11** (2001), 918–936.

[49] Q. Shan, J. Jia and A. Agarwala, High-quality motion deblurring from a single image, *ACM T. Graphic,* **27** (2008), p73.

[50] A. Shapiro, Sensitivity analysis of parameterized variational inequalities, *Math. Oper. Res.,* **30** (2005), 109–126.

[51] J. J. Ye, Necessary and sufficient optimality conditions for mathematical programs with equilibrium constraints, *J. Math. Anal. Appl.,* **307** (2005), 350–369.

[52] J. J. Ye, D. L. Zhu and Q. J. Zhu, Exact penalization and necessary optimality conditions for generalized bilevel programming problems, *SIAM J. Optim.,* **7** (1997), 481–507.

[53] Y.-L. You and M. Kaveh, A regularization approach to joint blur identification and image restoration, *IEEE Trans. Image Process.,* **5** (1996), 416–428.

E-mail address: hint@math.hu-berlin.de
E-mail address: wutao@math.hu-berlin.de